To die or not to die: early warnings of tree dieback in response to a severe drought

J. Julio Camarero[1,2*], Antonio Gazol[3], Gabriel Sangüesa-Barreda[3], Jonàs Oliva[4] and Sergio M. Vicente-Serrano[3]

[1]ARAID, Instituto Pirenaico de Ecología (IPE-CSIC). Avda. Montañana 1005, 50192 Zaragoza, Spain.

[2]Departament d'Ecologia, Universitat de Barcelona, Avda. Diagonal 645, 08028 Barcelona, Spain.

[3]Instituto Pirenaico de Ecología (IPE-CSIC). Avda. Montañana 1005, 50192 Zaragoza, Spain.

[4]Department of Forest Mycology and Plant Pathology, Swedish University of Agricultural Sciences, Box 7026, S-750 07 Uppsala, Sweden

Running headline: Is drought-induced dieback a critical transition?

*Corresponding author:

J. Julio Camarero

Instituto Pirenaico de Ecología (IPE-CSIC)

Avda. Montañana 1005, Apdo. 202

E-50192 Zaragoza, Spain.

E-mail: jjcamarero@ipe.csic.es

Tel.: (+34) 976 716031, Fax: (+34) 976 716019

Abstract

1. Some disturbances can drive ecological systems to abrupt shifts between alternative stages (tipping points) when critical transitions occur. Drought-induced tree death can be considered as a nonlinear shift in tree vigour and growth. However, at what point do trees become predisposed to drought-related dieback and which factors determine this (tipping) point? We investigated these questions by characterizing the responses of three tree species, silver fir (*Abies alba*), Scots pine (*Pinus sylvestris*) and Aleppo pine (*Pinus halepensis*), to a severe drought event.

2. We compared basal-area increment (BAI) trends and responses to climate and drought in declining (very defoliated and dying) versus non-declining (slightly or not defoliated) trees by using generalized additive mixed models. Defoliation, BAI and sapwood production were related to functional proxies of tree vigour measured at the onset and end of the drought (non-structural carbohydrate concentrations, needle N content and C isotopic discrimination, presence of wood-inhabiting fungi). We evaluated whether early-warning signals (increases in synchronicity among trees or in autocorrelation and standard deviation) could be extracted from the BAI series prior to tree death.

3. Declining silver fir and Scots pine trees showed less growth than non-declining trees one to three decades, respectively, before the drought event, whereas Aleppo pines showed growth decline irrespective of tree defoliation. At the end of the drought period, all species showed increased defoliation and a related reduction in the concentration of sapwood soluble sugars. Defoliation was constrained by the BAI of the previous five years and sapwood production. No specific wood-inhabiting fungi were found in post-drought declining trees apart from blue stain fungi, which extensively affected damaged Scots pines. Declining silver firs showed increases in BAI autocorrelation and variability prior to tree death.

4.   *Synthesis*. Early-warning signals of drought-triggered mortality seem to be species specific and reflect how different tree species cope with drought stress. Highly correlated declining growth patterns during drought can serve as a signal in silver fir, whereas changes in the content of sapwood soluble sugars are suitable vigour proxies for Scots and Aleppo pines. Longer growth and defoliation series, additional vigour parameters and multi-species comparisons are required to understand and predict drought-induced tree death.

Introduction

Forest dieback in response to warming-related drought illustrates some of the challenges that global change poses for ecologists (Allen *et al.* 2010). First, dieback may happen in response to previous constraints, including climate warming (Williams *et al.* 2013), that reduce tree vigour or growth in the long term (predisposing factors *sensu* Manion 1991). Therefore, we need new tools and approaches to quantify those long-term processes acting before drought-triggered mortality occurs (Pedersen 1998). Second, we have a limited (but rapidly growing) knowledge of the key physiological mechanisms responsible for dieback and tree mortality which restrains our ability to identify generalizable properties of the process. Current mechanistic approaches emphasize the interrelationships between carbon metabolism and plant hydraulics (McDowell *et al.* 2008, 2011). It is assumed that drought induces stomatal closure, leading to reduced photosynthesis and carbon starvation, whereas failure to close stomata may cause catastrophic xylem embolism of the vascular system, hydraulic failure and tree death through excessive water loss (Adams *et al.* 2013; Sevanto *et al.* 2014). Third, stress drivers interact and tree responses may be nonlinear. For instance, temperature rise could lead to a nonlinear increase in the growing-season vapour pressure deficit (atmospheric demand for moisture) and, thus, amplify the negative roles of warming and drought on tree mortality (Breshears *et al.* 2013).

Warmer temperatures and aridification trends portend increases in regional dieback events and background rates of tree mortality with positive feedbacks on climate warming through the reduction of land carbon sinks and canopy cover, and the loss of ecosystem services (Bonan 2008; Anderegg, Kane & Anderegg 2013). Therefore there is a pressing need to determine whether climate warming and increasing drought stress will increase the likelihood and extent of tree mortality. However, even determining when a tree dies is not an easy task (Anderegg, Berry & Field 2012). Here, we aim to gain a better understanding of

3

26   drought-triggered tree mortality by considering tree death as a nonlinear threshold of tree

27   vigour and growth (Fig. 1). This theoretical framework states that there are critical transitions

28   or tipping points beyond which ecological systems shift to alternative states (Scheffer *et al*.

29   2001). Such nonlinear thresholds are relatively abrupt and irreversible but it has been

30   proposed that tipping points can be preceded by detectable increases in the variability of the

31   system that can be used as early-warning signals (Dakos *et al*. 2012a, 2012b). For example,

32   climate warming and successive severe droughts should lead to growth decline, thus

33   triggering mortality; however, tree death could also be preceded by an increase in growth

34   persistence (autocorrelation) and variance. Indeed, several tree-ring studies have reported that

35   not only do dead trees usually have lower growth rates but that their growth also showed a

36   high variability and increased responsiveness to water deficit (Pedersen 1998; Ogle, Whitham

37   & Cobb, 2000; Bigler *et al*. 2006). However, even some generally assumed patterns show

38   exceptions because high growth rates in the past may predispose trees to drought-related

39   death (Jenkins & Pallardy 1995; Voltas *et al*. 2013). Hence, we need new approaches for

40   effective comparisons of past radial-growth trends of declining (very defoliated) and dead

41   trees versus non-declining (less defoliated) trees. Here, we retrospectively evaluate whether

42   those growth trends contain early-warning signals of drought-triggered mortality (critical

43   transition), namely low growth rates among declining or recently dead trees, an increase in

44   synchronicity among trees (considered a proxy of sensitivity to drought) and a rise in growth

45   autocorrelation and variability prior to tree death.

46   Using this statistical approach we aim to detect early-warning signals in growth series

47   of declining–dead versus non-declining trees. However, secondary growth is only a proxy of

48   carbon uptake and tree vigour (Fritts 2001). For that reason, we carry out a comprehensive

49   assessment of tree mortality by assessing several variables related to tree vigour (crown

50   defoliation, xylogenesis, concentrations of non-structural carbohydrates in sapwood and

51   needles, needle nitrogen concentrations and carbon isotope discrimination, and fungal

52   infection) at the onset and at the end of the severe drought in 2012, which affected several

53   conifer species across NE Spain. We characterize the responses to drought of three conifers

54   dominating areas subjected to different water deficits, ranging from relatively wet and cool

55   sites with forests of *Abies alba* Mill (silver fir), to continental *Pinus sylvestris* L. (Scots pine)

56   sites and semi-arid *Pinus halepensis* Mill. (Aleppo pine) woodlands. Specifically, we aim to:

57   (i) reconstruct and analyse the past and recent growth trends and responses to drought of co-

58   occurring declining and non-declining trees; (ii) relate those growth patterns with an

59   exhaustive description of vigour proxies that should reflect tree responses to drought-induced

60   dieback. We hypothesize that early-warning signals will be observed in the radial-growth

61   series prior to tree death such as previous growth decline, higher responsiveness to drought

62   and increased persistence and variance. We also hypothesize that drought should lead to a

63   defoliation-related reduction in non-structural carbohydrates in needles and sapwood. Finally,

64   we assess whether declining and dead trees showed symptoms of fungal infection (i.e.

65   whether fungal pathogens played a relevant role as drivers of tree death).

66

67   **Material and methods**

68   *Study site and species*

69   In early 2012, we selected three sites in NE Spain (Aragón) dominated by three different

70   conifer species: silver fir (*Abies alba*), Scots pine (*Pinus sylvestris*) and Aleppo pine (*Pinus*

71   *halepensis*). These sites were characterized by presenting abundant defoliated, dying or dead

72   trees of the dominant species (Supporting Information, Fig. S1). Such dieback coincided with

73   a severe drought that began the previous winter, as indicated by the minimum values of

74   monthly cumulative water deficit recorded during those months (Supporting Information, Fig.

75   S2). The study sites are subjected to Mediterranean and continental climatic conditions but

76   have contrasting water deficits based on climatic data obtained from nearby climatic stations

77   (see a summary of site, climate, soil and forest characteristics in Table 1). Furthermore, the

78   silver fir and Scots pine sites are located near the southernmost ("rear edge") limit of

79   distribution of the species (Supporting Information, Fig. S3). All the stands studied had not

80   been managed since the 1950s.

81   Silver fir and Scots pine are conifers that are dominant in temperate and continental

82   sites, whereas Aleppo pine is a Circum-Mediterranean conifer better adapted to withstand

83   summer drought in dry and semi-arid areas (Camarero *et al*. 2012). The three study species

84   show isohydric regulation of their water status by avoiding hydraulic failure through rapid

85   stomatal closure, causing a decrease of photosynthetic carbon uptake and potential depletion

86   of carbon reserves (Bréda *et al*. 2006). However, this strict stomatal control or "water-saving"

87   strategy can make isohydric plants that experience prolonged droughts of severe to

88   intermediate intensity more prone to carbon starvation and death (McDowell *et al*. 2008).

89

90   *Climate data and drought index*

91   We obtained monthly climatic variables [mean maximum and minimum temperatures,

92   precipitation (P), estimated potential evapotranspiration (PET) and water balance (P-PET)]

93   from meteorological stations located near the sampling sites for the period 1950−2012 (see

94   details on the climatic stations in Table 1). The time series of the climate variables were

95   carefully controlled and homogenized. The monthly PET was estimated using monthly values

96   of mean temperature, daily temperature range and extraterrestrial solar radiation following the

97   Hargreaves−Samani method (Hargreaves and Samani 1982). To quantify the impact of

98   drought on tree growth we used the multiscalar Standardized

99   Precipitation−Evapotranspiration Index (SPEI; see Vicente-Serrano, Beguería & López−

100 Moreno 2010). The use of the SPEI is relevant to quantify the effects of droughts on radial

101 growth at different time scales (see Fig. 2), as demonstrated in a study conducted in NE Spain

102 (Pasho *et al*. 2011) and using a global dataset (Vicente-Serrano *et al*. 2013). These studies

103 show that during dry periods (negative SPEI values) tree growth declines and that the

104 strongest growth responses to SPEI usually occur at different scales at dry compared with

105 mesic sites. To determine how extreme the 2012 drought was, we determined the return

106 period of the SPEI values according to the probability of the standard normal distribution.

107

108 *Field sampling*

109 At each study site, across a sampling area ranging from 0.5 ha (silver fir, Scots pine) to 2.0 ha

110 (Aleppo pine), we randomly selected 38 trees of the dominant tree species that were at least 5

111 m apart from each other. We mapped (*x* and *y* coordinates), tagged and measured size

112 variables in all trees (dbh, diameter at breast height measured at 1.3 m; height). To

113 characterize tree vigour we estimated the percentage of crown defoliation and mistletoe

114 (*Viscum album* L.) abundance (semi-quantitative scale) using binoculars (Dobbertin 2005;

115 Sangüesa-Barreda, Linares & Camarero 2013). Mistletoe was not observed in the Scots pine

116 stand. Given that crown defoliation estimates vary among observers and places, defoliation

117 data were always taken in 5% steps by the first author by comparing every tree with a

118 reference tree with the maximum amount of foliage at each site. Tree defoliation was assessed

119 in March (prior to bud burst) and August (when both primary and radial growth were mostly

120 finished) 2012, referred to hereafter as pre- and post-drought samplings. Trees showing <50%

121 post-drought defoliation were considered to be non-declining, whereas trees with ≥50% post-

122 drought defoliation were considered to be declining. The 50%-defoliation chriterion

123 represented a robust threshold to differentiate declining from non-declining trees based on

124 recent growth data (Supporting Information, Table S2). Dead trees were regarded as those

125 completely defoliated or having only red needles at the end of the drought. Declining and

7

126 dead trees were grouped together in further analyses because they showed similar defoliation

127 and growth trends. Given that both pine sites formed open stands we did not try to determine

128 the current competition-intensity index. Furthermore, tree-to-tree competition is not a

129 significant driver of silver-fir decline in Pyrenean sites (Camarero *et al.* 2011).

130

131 *Dendrochronological data*

132 We used dendrochronology to retrospectively characterize growth trends of trees (Fritts

133 2001). Secondary growth was measured by extracting one radial core per tree in late 2012 at

134 1.3 m using a Pressler increment borer. We considered one core sufficient to characterize

135 growth trends; so as to avoid damaging the monitored trees further (Woodall 2008). We

136 measured the length of the sapwood in the extracted cores in the field; in the case of silver fir,

137 we applied stain (bromocresol green) to distinguish the sapwood clearly. We calculated the

138 proportion of the core that was sapwood relative to the radius of the tree. Given the tight

139 relationship between the length of sapwood in the core and the proportion of the core that was

140 sapwood ($r = 0.82$-0.90, $P < 0.001$) we used the former in further analyses because it

141 produced similar results to those obtained using relative values. Wood samples were sanded

142 until tracheids were visible and then visually cross-dated. Once dated, we measured the tree-

143 ring widths to the nearest 0.01 mm using a binocular scope and a LINTAB measuring device

144 (Rinntech, Germany). The accuracy of visual cross-dating was checked with the program

145 COFECHA, which calculates moving correlations between each individual series and the

146 mean site series (Holmes 1983). We successfully dated and measured 35, 37 and 33 silver fir,

147 Scots pine and Aleppo pine trees, respectively. Tree growth measurements were derived by

148 converting the tree-ring width series into basal area increment (BAI) which accounts for the

149 geometrical constraint of adding a volume of wood to a stem of increasing radius (Biondi and

150 Qaedan 2008). We obtained the BAI by using the formula:

151
$$BAI = \pi \, (r_t^2 - r_{t-1}^2) \qquad\qquad (1)$$

152   where r_t and r_{t-1} are the squared stem radial increments at the end and the beginning of a given

153   annual ring increment corresponding to rings formed in years t and t-1, respectively. In the

154   case of cores without pith, we estimated the radius by fitting a geometric pith locator to the

155   innermost rings to calculate the length of the missing part of the radius (Duncan 1989).

156

157   *Xylogenesis*

158   Xylem phenology (xylogenesis) can be used to assess changes in tree vigour (Gričar, Krže &

159   Čufar 2009). To compare growth potential between declining and non-declining trees we

160   extracted wood microcores from the stem at a height of 1.0 m in 20 trees in spring (late May)

161   when high rates of xylem production occur in the study species (Camarero, Olano & Parras

162   2010; Cuny *et al.* 2012). Trees were randomly selected within the declining and non-declining

163   classes of each species; completely defoliated trees or trees without living needles were

164   excluded. Microcores were preserved in ethanol, transversally cut, and then stained to

165   differentiate xylem cells (radially enlarging, wall thickening and mature tracheids) according

166   to their colour and shape (indicating different developmental phases; for further details see

167   Camarero *et al.* 2010). The three types of tracheids were counted along five radial lines of the

168   2012 ring and mean values for each vigour class were obtained for the three species.

169

170   *Carbohydrate concentrations in sapwood and needles*

171   To assess carbon storage or mobilization we quantified the concentrations of non-structural

172   carbohydrates (NSC) in sapwood and current-year needles in the pre-drought (2011 needles)

173   and post-drought (2012 needles) samplings. Stem sapwood and needles account for the largest

174   proportion of total NSC pools in conifers and could be affected by crown defoliation (Fischer

175   and Höll 1991, Oleksyn *et al.* 2000). All samples were collected between 10.00 h and 13.00 h

176   to avoid diurnal variability in NSC concentrations. Current-year needles were collected from

177   two upper and light-exposed branches from each tree with green foliage. Stem sapwood

178   samples were obtained by taking two radial core samples per tree at 1.3 m using a Pressler

179   increment borer. Needle and wood samples were transported to the laboratory in a portable

180   cooler. Needles were dried in the oven at 60ºC for 72 h. Portions of sapwood (outer 5 cm)

181   were separated from each core using a razor blade. Wood samples were subsequently frozen

182   and stored at -20 ºC until freeze dried. All dried samples were weighted and milled to a fine

183   powder in a ball mill (Retsch Mixer MM301, Leeds, UK) prior to chemical analyses. Soluble

184   sugars (SS) were extracted with 80% (v/v) ethanol and their concentration determined

185   colorimetrically using the phenol-sulfuric method of Dubois *et al*. (1956) as modified by

186   Buysse and Merckx (1993). Starch and complex sugars remaining after ethanol extractions

187   were enzymatically reduced. NSCs measured after ethanol extraction are referred to as

188   soluble sugars (SS) and carbohydrates measured after enzymatic digestion are referred to as

189   starch. The sum of SS and starch is referred to as NSC.

190

191   *Needle nitrogen and carbon isotope discrimination*

192   We measured needle nitrogen (N) and carbon isotope discrimination (δ^{13}C) in the post-

193   drought samples. Needle N and δ^{13}C were used as surrogates of nutrient use and integrated

194   water-use efficiency (i.e. the amount of carbon gained per unit of water lost) (Farquhar,

195   Ehleringer & Hubick 1989). Samples of current-year needles from all trees with green foliage

196   in late summer were obtained and ground as already described. Needle N concentration was

197   measured using an elemental analyser (VarioMAX, Hanau, Germany); needle δ^{13}C was

198   analysed at the Stable Isotope Facility (University of California, Davis, USA) using an

199   isotope-ratio mass spectrometer (Thermo Finnigan MAT 251, Bremen, Germany). The

200   relationship between carbon stable isotopes was expressed in relation to a Pee-Dee Belemnite

201   (PDB) standard. The accuracy of the δ^{13}C measurements was 0.05‰.

202

203   *Wood-inhabiting fungi*

204   To detect the presence of wood-inhabiting fungi associated with the dieback, we took two

205   core samples per tree from the stump and the upper main root of every tree in autumn 2012

206   using a Pressler increment borer. The borer was carefully sterilized after the extraction of

207   each core using ethanol 70%. Increment cores were placed in sterile plastic tubes, transported

208   to the laboratory within two days of extraction, stored at 4º C and plated out onto selective

209   media within the next three days. Based on observations in previous studies of silver fir

210   decline (Oliva & Colinas 2007), we attempted to isolate the root-rot fungi *Armillaria* and

211   *Heterobasidion* from silver fir cores by plating the cores onto malt-extract-based selective

212   media for basidiomycetes that included benomyl (10 mg l^{-1}) and chloramphenicol (200 mg

213   l^{-1}). Cores were incubated at 20–22°C in the dark and observed weekly for a period of three

214   months. Fungal colonies growing from the cores were transferred onto malt agar plates.

215   Fungal identification was performed by extracting DNA, amplifying the internal transcribed

216   spacer region, sequencing and performing BLAST searches in the GenBank and UNITE

217   databases (Benson *et al*. 2013, Kõljalg *et al*. 2005). We used 98% as a similarity threshold for

218   typing our sequences at species level. The wood samples of both pine species showed signs of

219   discoloration, particularly the Scots pine samples, which showed signs of blue stain fungi.

220   Owing to the potential involvement of blue stain ascomycetes, the selective media onto which

221   the pine cores were plated did not include benomyl. To obtain a quantitative measure of the

222   damage caused by sap stain in Scots pine, we measured the extent of blue stain in the

223   increment core from which we extrapolated the proportion of the section that was colonized

224   (Heiniger *et al*. 2011).

226   *Interrelationships between vigour proxies and dieback*

227   We used Structural Equation Models (hereafter SEMs) to explore multiple pathways and

228   proxies related to tree dieback (defoliation, bai decline, NSC, needle chemical variables). In

229   SEMs, researchers may enter information a priori and reformulate the models using goodness-

230   of-fit statistics, which enables the use of both deductive and inductive approaches (Bollen

231   1989). The SEM approach is based on a general linear model and enables the simultaneous

232   assessment of direct and indirect relationships among variables (Grace 2006). SEMs can test

233   hypotheses involving multiple relationships between the studied variables (standardized

234   partial regression coefficients or path coefficients) expressed as structural equations. These

235   equations can be represented in a "path" diagram where the variables are connected by arrows

236   representing the theoretical structural model for the system under consideration. In this study,

237   SEMs were used as a confirmatory statistical method because we tested how our dataset

238   resembled a knowledge-based theoretical model.

239   We developed an a priori conceptual model of dieback (Fig. 3a). We hypothesized that

240   the post-drought defoliation occurred as a result of a decline in growth in previous years (i.e.

241   the mean BAI for 2008−2012 was selected after preliminary analyses and abbreviated as

242   bai5), diminished sapwood production and reduced sapwood or needle NSC concentrations

243   (carbon depletion used to rebuild the crown), which were positively associated. A decline in

244   growth in previous years, sapwood production and wood or needle NSC concentrations could

245   indicate a lower ability of trees to tolerate further drought stress because of a loss in hydraulic

246   efficiency and impaired carbon uptake and transport (Ryan and Yoder 1997; McDowell *et al*.

247   2008). Defoliation could also lead to an increase in needle N due to declining primary growth

248   (concentration effect) and a decrease in needle $\delta^{13}C$ and water-use efficiency as a

249   consequence of stomata opening and excessive water loss through needles (McDowell *et al*.

250   2008; Galiano, Martínez-Vilalta & Lloret 2011). Scatter plots and Pearson correlation

251   analyses were used to analyse bivariate relationships between the considered variables. The *t*-

252   test was also used to assess the statistical significance of differences between declining and

253   non-declining trees in the study variables. Most of the variables compared followed normal

254   distributions (dbh, height, sapwood area, age, sapwood SS concentrations, no. of expanding

255   tracheids), and those departing from a normal distribution were log-transformed to reach

256   normality (bai 2008−2012, defoliation). A separate SEM was fitted for each species. The

257   overall fit of the model (i.e. the comparison of observed versus model-implied covariances

258   using a maximum likelihood-based minimization process) leads to the selection of parameter

259   estimates and produces a global assessment of the model, here quantified using the χ^2 statistic

260   and its associated probability level (*P*), and the Goodness of Fit Index (GFI). A high *P* value

261   and a GFI > 0.90 indicate an acceptable fit for the model (Grace 2006). We used the Amos

262   software to calculate SEMs (Arbuckle 2010).

263

264   *Growth trends and response to climate in declining and non-declining trees*

265   We used Generalized Additive Mixed Models (GAMM; Wood 2006) to study the long-term

266   BAI trends and responses to drought of declining and non-declining trees of the three study

267   species. GAMM is a semi-parametric method that allows the simultaneous modelling of linear

268   and nonlinear relationships between the response variable (here BAI) and the different

269   covariates by using regression splines. Several GAMM models were fitted and compared.

270   First, we studied the presence of non-linear growth trends and the influence of tree ontogeny

271   (represented by age), size (dbh) and the spatial structure (*x* and *y* coordinates). For each

272   species, we applied a GAMM of the form:

273             $\log(\mathrm{BAI}_i+1) = s(\mathrm{dbh}_i) + s(\mathrm{age}_i) + s(\mathrm{year}) + te(x,y) + Z_iB_i + \upsilon_i$ (2)

274   where the BAI of a tree *i* is modelled as smooth functions (*s*) with different combinations of

275   the four predictors. In addition, given that BAI represents multiple measurements performed

276   in each tree, tree identity ($Z_i B_i$) is regarded as a random effect (Z_i and B_i indicate matrix

277   variables and related coefficients). For dbh, age and year, smooth terms were represented

278   using smooth splines with default package settings, whereas in the case of the spatial

279   coordinates a tensor product (*te*) spline was used (Augustin *et al*. 2009). Given that BAI has a

280   skewed distribution, we log-transformed this variable (log x +1). In addition, we also included

281   an error term (υ_i) in the model with a first-order temporal autocorrelation [AR(1)] structure.

282   Eight potential models were calculated and ranked according to their second-order Akaike

283   information criterion (AICc). The model with the lowest AICc was selected (Burnham and

284   Anderson, 2002).

285   In a second step, we included the differences in growth between declining and non-

286   declining trees and the potential influence of drought on BAI. Specifically, we considered

287   nine GAMMs by including a factor classifying trees as declining and non-declining, the SPEI

288   June drought index, and potential interactions between these variables and the non-linear

289   trends in tree growth. For each tree species, we fitted a GAMM of the form:

290    $\log(\mathrm{bai}_i+1) = s(\mathrm{dbh}_i) + s(\mathrm{age}_i) + s(\mathrm{year}*\mathrm{declining}) + te(x,y) + \mathrm{drought}*\mathrm{declining} + Z_i B_i + \upsilon_i$ (3)

291   which models bai considering different responses to drought in declining and non-declining

292   trees of each species. Again, models were calculated and ranked according to their AICc and

293   the one with the lowest AICc was selected. The GAMMs were performed using the function

294   *gamm* in the *mgcv* package (Wood 2011).

295

296   *Tipping points and tree dieback*

297   We used several statistical techniques to evaluate whether critical transitions can be detected

298   in a growth series before tree dieback occurs. Recent studies have suggested that the

299 proximity of a system or an organism to a tipping point (critical transition to a new state) is

300 preceded by early-warning signals that can be detected using time series analyses (Dakos *et*

301 *al*. 2012a). In particular, mathematical properties such as the AR(1) or the standard deviation

302 (SD) of a time series representing temporal trends of a natural system may vary near to a

303 tipping point and can be used as "early warnings". In natural systems, slowing down can be

304 an indicator of changes in the system and can be represented by an increase in AR(1) or

305 variance (SD) near the tipping point (Dakos *et al*. 2012b). We also quantified tree-to-tree

306 synchronicity in growth, which should increase in response to drought stress (Fritts 2001).

307   We explored the presence of early warning signals in the growth trends of declining

308 and non-declining trees of the three species studied. First, we studied tree growth

309 synchronicity of declining and non-declining trees of each species. The mean Pearson

310 moment correlation coefficient (*r*) between all pairs of individual bai series was calculated

311 using moving 30-year-long time windows displaced every year starting in 1950. This was

312 done separately for declining and non-declining trees of the three species as a measure of

313 growth synchronicity within each vigour class. These correlations were plotted against year to

314 detect trends (quantified using *r*) or sudden changes in growth synchronicity. Second, we

315 quantified the AR (1) and the SD of residuals of the mean bai series of declining and non-

316 declining trees of each species. The mean bai series for each vigour class and species were

317 log-transformed and detrended applying a Gaussian filtering that was half the size of the time

318 period studied (30 years). The mean series of BAI residuals were then analysed using 30-

319 year-long moving windows. The nonparametric Kendall τ statistic was used to analyse the

320 trends of AR(1) and SD because it is a robust statistic against the presence of heterogeneity in

321 a time series. The Kendall τ statistic measures the strength of the trend by comparing the

322 ranks of the time data and the analysed variable reaching maximum and minimum values of

323 +1 and −1, respectively. If the variable increases as time advances then $\tau > 0$, whereas a

324 negative τ value indicates a decreasing trend. The analyses were performed using the

325 functions provided in the *earlywarnings* package (Dakos *et al.* 2012a). All statistical analyses

326 were performed using the R statistical software (R Development Core Team, 2014).

327

328 **Results**

329 *Growth responses to the extreme drought*

330 The 5- and 10-month-long SPEIs calculated in June 2012 for the silver fir, Scots and Aleppo

331 pine sites were, respectively, −2.40, −1.90 and −1.92, respectively, corresponding to drought

332 return periods of 122, 35 and 36 years, in that order. Therefore, these low SPEI values

333 represent extreme dry conditions for the period 1950−2012 (Supporting Information, Fig. S4).

334 We were able to successfully cross-date most tree-ring series to determine the highest

335 and lowest mean growth rates in silver fir and Scots pine, respectively (Supporting

336 Information, Table S1). On average, silver fir showed the lowest autocorrelation in radial

337 growth whereas Scots pine had the highest coherence among trees and also the maximum

338 year-to-year variability in ring width. The June SPEI was the climatic variable most tightly

339 related to BAI when considering the three species (Fig. 2, Supporting Information, Fig. S5);

340 however, this association was observed for longer time scales (10 month) at the driest site (*P.*

341 *halepensis*) and for shorter time scales (5 months) at the other two sites (*A. alba*, *P.*

342 *sylvestris*).

343

344 *Differences between declining and non-declining trees*

345 Declining−dead and non-declining trees only differed in terms of crown defoliation, sapwood

346 production, post-drought sapwood SS concentration and bai5, with significantly higher values

347 for non-declining trees except in the case of defoliation (Table 2). The rest of the analysed

348 variables did not show any significant difference between vigour classes (results not shown).

349   Overall, all trees produced a low number of expanding tracheids, indicating a low growth

350   potential except for the non-declining silver firs. In spring, a significantly lower number of

351   expanding tracheids were produced by declining trees compared with the non-declining trees

352   in all species (Table 2). The other tracheid types were not significantly different (results not

353   shown). Declining trees showed a greater response to water balance during the critical months

354   for growth (spring, previous autumn) than the non-declining trees (Supporting Information,

355   Fig. S5)

356

357   *Drivers and proxies of defoliation*

358   In all species, the strongest negative associations were observed between sapwood

359   production, post-drought sapwood SS concentration and defoliation (Figs. 3 and 4). Indeed,

360   pre-drought defoliation and sapwood SS abundance were also inversely related except in the

361   case of Scots pine trees (Fig. 4). We found higher post-drought than pre-drought sapwood SS

362   concentrations in the case of silver fir and Aleppo pine; however, these differences were not

363   significant (silver fir, $F = 3.07$, $P = 0.08$; Aleppo pine, $F = 0.74$, $P = 0.39$). The selected

364   SEMs, which accounted for more than 50% of the variance in tree defoliation, indicated that

365   the effect of sapwood on defoliation was direct in the case of silver fir (Fig. 3b), whereas in

366   Aleppo pine, sapwood had an indirect effect on defoliation through reduced sapwood SS

367   concentrations, and in Scots pine defoliation was mainly driven by sapwood SS (Fig. 3c and

368   3d). Previous BAI (bai5) was the second most important variable explaining current

369   defoliation after sapwood variables, with a significant negative effect in both pine species but

370   not in silver fir. Sapwood production was significantly and positively related to bai5 in all

371   species except Aleppo pine.

372   In Scots pine, the post-drought defoliation was positively related to needle SS

373   concentrations ($r = 0.34$, $P = 0.04$) but negatively associated with needle starch

17

374 concentrations ($r = -0.57$, P <0.001). In Scots and Aleppo pines, post-drought defoliation and

375 needle N concentration were positively ($r = 0.34$, $P = 0.03$) and negatively ($r = -0.32$, $P =$

376 0.04) related, respectively. Defoliation was unrelated to needle δ^{13}C, which only showed a

377 positive association with post-drought sapwood starch concentration in Aleppo pine ($r = 0.37$,

378 $P = 0.03$). In spite of these aforementioned relationships, no needle chemical variable (NSC,

379 N and δ^{13}C) entered into the selected SEMs.

380

381 *Role of forest pathogens*

382 Scots pine was predominantly damaged by blue-stain fungi. The proportion of the blue

383 stained area at stump level was positively related to post-drought defoliation ($r = 0.54$, P

384 <0.001) and negatively associated with sapwood SS concentrations (Fig. 5a). We could not

385 isolate the causal agent from all affected trees; however, four trees appeared to be infected by

386 the blue stain fungus *Ophiostoma minus* (Hedgcock) Sydow et P. Sydow. Other fungi isolated

387 from Scots pine wood were *Umbelopsis isabellina* (Oudem.) W. Gams and *Acremonium*

388 *strictum* W. Gams. In the case of Aleppo pine, the heart-rot fungus *Porodaedalea pini* (Brot.)

389 Murrill was the predominant pathogen, although no association with defoliation or carbon

390 reserves could be found. In the case of silver fir, the dominant pathogen was *Amylostereum*

391 *chailletii* (Pers.) Boidin, which was isolated from five dying silver fir trees. Other pathogens

392 such as *Heterobasidion annosum* (Fr.) Bref. s.l., *Ganoderma lucidum* (Curtis) P. Karst. and

393 *Trichaptum abietinum* (J. Dicks.) Ryvarden were only isolated from two trees each.

394 *Amylostereum*-infected trees had lower starch and SS sapwood concentrations than non-

395 declining trees in the pre- and post-drought periods, respectively (Fig. 5b).

396

397 *Growth trends*

18

398   The GAMMs revealed different BAI trends for the three species studied (Fig. 6, Table 3). The

399   non-linear trend was present in the models of all three species (Fig. 6), whereas tree size (dbh)

400   was only selected in the models of Scots pine and silver fir, and ontogeny (tree age) was only

401   significant in the case of Scots pine (Table 3). The spatial location of trees did not have an

402   influence on BAI trends (Supporting Information, Table S3).

403   The BAI trends of declining and non-declining trees started to diverge in the mid-

404   1990s in the case of silver fir and in the 1980s in the case of Scots pine (Fig. 6). In Aleppo

405   pine, both declining and non-declining have shown a growth loss since the 1980s. Indeed,

406   only in this species were defoliation and the year of cambial death (the last formed tree-ring)

407   significantly associated ($r = -0.59$, $P = 0.001$), indicating the long-term decline of these trees.

408   For example, the most defoliated trees stopped growing on average seven years before the

409   sampling year, whereas the least defoliated trees only stopped growing two years before the

410   sampling. The second selected GAMM, incorporating different BAI responses of declining

411   and non-declining trees to drought stress, demonstrated that drought is an important driver of

412   long-term BAI trends for the three study species (Fig. 6, Table 4). The models revealed that

413   the BAI response to drought in declining and non-declining trees of both pine species differed

414   but did not differ among silver fir trees (Table 4), suggesting that factors driving growth

415   decline are species specific.

416

417   *Early-warning signals of tree dieback and death*

418   The analyses of BAI performed to detect early warnings of tree dieback showed contrasting

419   results depending on the species (Fig. 7). In silver fir, there was a coherent inflection point in

420   bai data indicating a rise in synchronicity among trees, AR(1) and SD after the 1995 drought.

421   These increases in synchronicity, autocorrelation and variance were higher for declining than

422   for non-declining trees even though the trends of those variables were negative for the whole

423   study period. A similar pattern was observed in Aleppo pine with increases in synchronicity,

424   AR(1) and SD following the 2005 drought, particularly in the case of declining trees. By

425   contrast, declining Scots pines showed a loss in synchronicity and decreases in AR(1) and SD.

426

427   **Discussion**

428   *Implications on the use of early-warning signals in growth series to portend die-off*

429   We found mixed results concerning the trees' growth responses to drought. Early-warning

430   signals in the growth series of declining trees prior to their death were detected in silver fir

431   (Fig. 7). Growth trends of declining and non-declining trees diverged in all species except

432   Aleppo pine (Fig. 6). First, declining Scots pine trees have shown a lower growth rate relative

433   to non-declining trees since the 1980s, which was a warm and dry decade (Fig. 6). In this

434   species, the low growth rates and high defoliation and blue-stain levels (Table 2, Fig. 5a), the

435   high levels of synchronicity in growth among trees and responsiveness to drought, and the

436   lack of clear early-warning signals suggest that the whole Scots pine study population is

437   experiencing a chronic drought-induced decline and may be prone to disappear. This could be

438   a paradigmatic case of a warming-induced ongoing local extinction of a rear-edge population

439   triggered by drought. Second, in Aleppo pine, growth trends declined irrespective of recent

440   tree defoliation (Figs. 2 and 6). Cambial death was common in this stand during the past

441   decade which implies an active selection of drought-tolerant non-defoliated trees. Cambial

442   death (i.e. when tree-ring production ceases) precedes total crown defoliation by several years

443   or even decades (Pedersen 1998). Therefore, the extensive growth decline of Aleppo pines

444   portends increasing defoliation and mortality levels in the forthcoming years. Third, the silver

445   fir growth series offered the best opportunity to use early-warning grow0th indicators of

446   dieback. In this species the divergence between vigour classes coincided with a severe

447   drought in 1995 (Fig. 6) and a sharp increase in autocorrelation and variability of all trees,

448 particularly declining trees (Fig. 7). Given that declining and non-declining silver firs showed

449 similar growth responses to drought, this population could also be experiencing a long-term

450 decline characterized by the removal of drought-intolerant defoliated individuals. Several

451 Pyrenean silver fir populations subjected to sub-optimal conditions are experiencing ongoing

452 decline and high mortality rates as temperatures rise and atmospheric water demand increases

453 (Camarero *et al.* 2011). Overall, our findings concur with previous studies showing how

454 growth is nonlinearly impacted by drought (Cavin *et al.* 2013). Such threshold responses in

455 growth and vigour suggest that warmer air temperatures may exacerbate drought stress in the

456 three study species by amplifying atmospheric water demand or the duration of the water-

457 deficit period (Peguero-Pina *et al.* 2007, Linares & Camarero 2012, Alexou 2013, Poyatos *et*

458 *al.* 2013).

459   Relative growth rates and short-term growth trends prior to tree death have been

460 shown to be reliable predictors of timing of tree death in Swiss *Picea abies* (L.) Karst.

461 (Norway spruce) forests (Bigler & Bugmann 2004) and in German *Fagus sylvatica* L. (beech)

462 stands (Gillner *et al.* 2013) among others. Here we show that considering autocorrelation and

463 variability prior to tree death improves our knowledge of the already complex mortality

464 processes in silver fir and Aleppo pine. We argue that a broad comparison of a long-term

465 growth series prior to death between dead, declining and non-declining trees of several tree

466 species from contrasting biomes would give a better insight about mortality patterns and

467 processes. The evaluation of tree death as a tipping point in vigour could profit from the

468 theoretical framework offered by ecological early-warning growth signals of increased

469 synchronicity and critical slowing down (e.g., Boden *et al.* 2014).

470   It is possible that our hypothesis referred to a defoliation-related reduction in needle

471 and sapwood NSC concentrations (Figs. 3 and 4). At the end of the drought period, all species

472 showed a defoliation-related reduction in the concentration of sapwood SS (Fig. 4). We also

473   observed increasing post-drought sapwood SS concentrations in the case of Aleppo pine, and

474   particularly silver fir, irrespective of tree defoliation (Fig. 4). Apparently, this could contradict

475   the isohydric behaviour of these species, which rapidly close stomata and reduce carbon

476   uptake to avoid hydraulic failure. However, we interpret such accumulation of sapwood SS as

477   a response to drought-induced declining sink activity (Sala *et al*. 2010), which would be most

478   relevant in silver fir. In addition, an increased concentration of sugars, derived from starch

479   stored in parenchyma cells, has been linked to the refilling of embolized vessels (Secchi &

480   Zwieniecki 2012). Interestingly, previous growth and sapwood production predetermined the

481   final levels of defoliation, which can be regarded as a multiannual process (Fig. 3). Given that

482   SS are among the most drought-responsive metabolites, their concentration changes could

483   reflect either an impairment of photosynthetic carbon uptake or a reduction in starch

484   hydrolysis. In Scots pine, the concentration of SS in needles increased and starch decreased as

485   response to defoliation, suggesting an active release of these molecules, which could represent

486   an early-warning stress signal to trees given that SS correlate negatively with leaf

487   photosynthesis (Franck *et al*. 2006) and act as osmoprotectants during water deficit stress

488   (Rodriguez-Calcerrada *et al*. 2011). We speculate that the general reduction of sugars in the

489   stem sapwood could be linked to an increase in the abundance of these metabolites in the

490   needles; however, but this association was only detected in Aleppo pine ($r = -0.39$, $P = 0.02$).

491   Thus, the negative effect of drought on sugar concentrations can have multiple and complex

492   effects and does not necessarily imply a link between tree death and carbon starvation (Sala,

493   Piper & Hoch 2010; Dietze *et al*. 2014). For instance, rapid death due to hydraulic failure may

494   be associated with a lack of adequate tissue carbohydrate content required for osmoregulation

495   owing to shifts in carbon allocation priorities or phloem dysfunction (Sevanto *et al*. 2014). In

496   addition, drought-triggered defoliation can lead to carbon depletion of roots in conifers

497   (Oleksyn *et al*. 2000; Hartmann, Ziegler & Trumbore 2013) while above-ground tissues use

498   sugars for osmorregulation or to rebuild the crown (Saffell *et al*. 2014). Overall, our findings

499   confirm that the sapwood concentrations of SS reflect crown defoliation in the two pine

500   species whereas needle chemical variables (NSC, N, δ^{13}C) do not.

501   In Scots pine, the decline in sapwood sugar content was not only linked to crown

502   defoliation but also to the abundance of blue-stain fungi in the wood (Fig. 5a). These

503   symptoms confirm that this population of trees was in decline and highlight the value of

504   combining defoliation and incidence of blue-stain fungi as early-warning indicators of forest

505   decline. Blue-stain fungi may be important contributing factors (*sensu* Manion 1991) involved

506   in the long-term decline of Scots pine populations, as demonstrated by Heiniger *et al*. (2011)

507   and theoretically proposed in Oliva, Stenlid & Martínez-Vilalta (2014). In silver fir, we could

508   not associate the susceptibility of trees to drought stress with previous fungal infection

509   because few trees were infecte with the same pathogen species (Fig. 5b). Given that

510   pathogens take a long time to kill a tree and the diversity of pathogens that attack trees, future

511   studies studies should use broader sampling designs than the one used in this study. For

512   instance, the presence of *H. annosum* and *Armillaria* spp. has not only been linked to dieback

513   but also to thinning in Pyrenean silver fir stands (Oliva & Colinas 2007; Oliva, Suz & Colinas

514   2009). Unlike previous findings in *Pinus mugo* Turra infected by *H. annosum*, which died

515   rapidly, possibly because of fungal attack (Cherubini *et al*. 2002), the declining silver firs in

516   this study, with or without fungal infection, presented diverse growth patterns.

517

518   *Species-specific responses of tree species to drought-induced die-off*

519   Statistical rarity was one aspect of the severe 2012 drought, which was characterized by low

520   levels of precipitation, a long dry period and also high temperatures. However, such an

521   unusual climatic episode was also an ecological extreme event (*sensu* Smith 2011) given that

522   the trees' responses were outside the typical or normal variability of the system. Our study

523 can be described as "opportunistic" (*sensu* Smith 2011) since we evaluated the trees'

524 responses to a climate extreme (2012 drought) during the course of an ongoing observational

525 study. Using a retrospective approach as we did can still capture large spatial and temporal

526 scale information, even though we cannot control for characteristics of climatic extremes

527 (type, timing, magnitude) or for other interacting factors (e.g., previous droughts). The length

528 of the 2012 drought exceeded the ability of the trees to tolerate drought stress leading to long-

529 term impacts such as ongoing defoliation, growth decline, mortality and changes in the

530 abundance of the dominant tree species. Such drought-triggered community shifts will have

531 cascading effects on forest composition and ecosystem services. Early-warning signals such

532 as an increase in growth persistence and variability were useful as death forecasts for silver fir

533 (Fig. 7), whereas the two pine species presented other dieback prognoses and responses to

534 defoliation (decrease in sapwood production and SS concentrations, blue-stain fungi). Future

535 dieback assessments could focus on those idiosyncratic proxies to determine the vulnerability

536 and resilience of forests in response to warming and drought stress. We suggest that more

537 attention should be focussed on the interactions between growth, defoliation and sapwood

538 function (including NSC use and transport) to forecast dieback and mortality as a function of

539 drought stress using process-based models. Finally, these simulation exercises could be scaled

540 up to the ecosystem level by using, for instance, ecohydrological models to evaluate the

541 extent to which drought-induced dieback and the resulting loss of canopy cover lead to:

542 decreased evapotranspiration and carbon sink potential, increased streamflow, and altered

543 water yield as a function of site aridity and post-mortality successional dynamics.

544

552 **References**

553 Adams, H. D., Germino, M. J., Breshears, D. D., Barron–Gafford, G. A., Guardiola–

554   Claramonte, M., Zou, C.B. & Huxman, T.E. (2013) Nonstructural leaf carbohydrate

555   dynamics of *Pinus edulis* during drought-induced tree mortality reveal role for carbon

556   metabolism in mortality mechanism. *New Phytologist*, **197**, 1142–1151.

557 Alexou, M. (2013). Development-specific responses to drought stress in Aleppo pine (*Pinus*

558   *halepensis* Mill.) seedlings. *Tree Physiology*, **10**, 1030–1042.

559 Allen, C.D., Macalady, A.K., Chenchouni, H., Bachelet, D., McDowell, N., Vennetier, M. et

560   al. (2010) A global overview of drought and heat-induced tree mortality reveals emerging

561   climate change risks for forests. *Forest Ecology and Management*, **259**, 660–684.

562 Anderegg W.R.L., Berry J.A. & Field C.B. (2012) Linking definitions, mechanisms, and

563   modeling of drought-induced tree death. *Trends in Plant Science*, **17**, 693–700.

564 Anderegg, W.R.L., Kane J. & Anderegg, L.D.L. (2013) Consequences of widespread tree

565   mortality triggered by drought and temperature stress. *Nature Climate Change*, **3**, 30–36.

566 Arbuckle, J.L. (2010) *IBM SPSS Amos 19 User's Guide*. IBM SPSS, Chicago.

567 Augustin, N.H., Musio, M., von Wilpert, K., Kublin, E., Wood S.N. & Schumacher, M.

568   (2009) Modeling spatiotemporal forest health monitoring data. *Journal of the American*

569   *Statistical Association*, **104**, 899–911.

570 Benson, D.A., Cavanaugh, M., Clark, K., Karsch-Mizrachi, I., Lipman, D.J., Ostell, J. &

571   Sayers, E.W. (2013) GenBank. *Nucleic Acids Research*, **41**, D36–D42.

572 Bigler, C., Bräker, O.U., Bugmann, H., Dobbertin, M. & Rigling, A. (2006) Drought as an

573   inciting mortality factor in Scots pine stands of the Valais, Switzerland. *Ecosystems*, **9**,

574   330–343.

575 Bigler, C. & Bugmann, H. (2004) Predicting the time of tree death using dendrochronological

576   data. *Ecological Applications*, **14**, 902–914.

577 Biondi, F. & Qaedan, F. (2008) A theory-driven approach to tree-ring standardization:

578   Defining the biological trend from expected basal area increment. *Tree-Ring Research*,

579   **64**, 81–96.

580 Bollen, K.A. (1989) *Structural Equations with Latent Variables*. Wiley, New York.

581 Bonan, G.B. (2008) Forests and climate change: forcings, feedbacks, and the climate benefits

582   of forests. *Science*, **320**, 1444–1449.

583 Boden, S., Kahle, H.-P., von Wilpert, K. & Spiecker, H. (2014) Resilience of Norway spruce

584   (*Picea abies* (L.) Karst) growth to changing climatic conditions in Southwest Germany.

585   *Forest Ecology and Management*, **315**, 12–21.

586 Bréda, N., Huc, R., Granier, A. & Dreyer, E. (2006) Temperate forest trees and stands under

587   severe drought: a review of ecophysiological responses, adaptation processes and long-

588   term consequences. *Annals of Forest Science*, **63**, 625–644.

589 Breshears, D.D., Adams, H.D., Eamus, D., McDowell, N.G., Law, D.J., Will, R.E., Williams,

590   A.P. & Zou, C.B. (2013) The critical amplifying role of increasing atmospheric moisture

591   demand on tree mortality and associated regional die-off. *Frontiers in Plant Science*, **4**,

592   266.

593 Buysse, J. & Merckx, R. (1993) An improved colorimetric method to quantify sugar content

594   of plant tissue. *Journal of Experimental Botany*, **44**, 1627–1629.

595 Burnham, K.P. & and Anderson, D.R. (2002) *Model Selection and Multimodel Inference*.

596   Springer, New York.

597 Camarero, J.J., Olano, J.M. & Parras, A. (2010) Plastic bimodal xylogenesis in conifers from

598   continental Mediterranean climates. *New Phytologist*, **185**, 471–480.

599 Camarero, J.J., Bigler, C., Linares, J.C. & Gil-Pelegrin, E. (2011) Synergistic effects of past

600   historical logging and drought on the decline of Pyrenean silver fir forests. *Forest Ecology*

601   *and Management*, **262**, 759–769.

602   Camarero, J.J., Sangüesa-Barreda, G., Alla, A.Q., González de Andrés, E., Maestro-Martínez,

603   M. & Vicente-Serrano, S.M. (2012) Los precedentes y las respuestas de los árboles a

604   sequías extremas pueden revelar los procesos involucrados en el decaimiento del bosque.

605   *Ecosistemas*, **21**, 22–30.

606   Cavin, L., Mountford, E.P., Peterken, G. F. & Jump, A.S. (2013) Extreme drought alters

607   competitive dominance within and between tree species in a mixed forest stand.

608   *Functional Ecology*, **27**, 1424–1435.

609   Cherubini, P., Fontana, G., Rigling, D., Dobbertin, M., Brang, P. & Innes, J.L. (2002) Tree-

610   life history prior to death: two fungal root pathogens affect tree-ring growth differently.

611   *Journal of Ecology*, **90**, 839–850

612   Cuny, H.E., Rathgeber, C.B.K., Lebourgeois, F., Fortin, M. & Fournier, M. (2012) Life

613   strategies in intra-annual dynamics of wood formation: example of three conifer species in

614   a temperate forest in north-east France. *Tree Physiology*, **32,** 612–625.

615   Dakos, V., Carpenter, S.R., Brock, W.A., Ellison, A.M., Guttal, V., Ives, A.R., Kéfi, S.,

616   Livina, V., Seekell, D.A., van Nes, E.H. & Scheffer, M. (2012a) Methods for detecting

617   early warnings of critical transitions in time series illustrated using simulated ecological

618   data. *PLoS One*, **7,** e41010. doi:10.1371/journal.pone.0041010

619   Dakos, V., Van Nes, E.H., D'Odorico, P. & Scheffer, M. (2012b) Robustness of variance and

620   autocorrelation as indicators of critical slowing down. *Ecology*, **93**, 264–271.

621   Dietze, M.C., Sala, A., Carbone, M.S., Czimczik, C.I., Mantooth, J.A., Richardson, A.D. &

622   Vargas, R. (2014) Nonstructural carbon in woody plants. *Annual Review of Plant Biology*,

623   **65**, 667–687.

624   Dobbertin, M. (2005) Tree growth as indicator of tree vitality and of tree reaction to

625   environmental stress: a review. *European Journal of Forest Research*, **124**, 319–333.

626   Dubois, M., Gilles, K.A., Hamilton, J.K., Rebers, P.A. & Smith, F. (1956) Colorimetric

627   method for determination of sugars and related substances. *Analytical Chemistry*, **28**, 350–

628   356.

629   Duncan, R.P. (1989) An evaluation of errors in tree age estimates based on increment cores in

630   Kahikatea (*Dacrycarpus dacrydioides*). *New Zealand Natural Sciences*, **16**, 31–37.

631   Farquhar, G.D., Ehleringer, J.R. & Hubick, K.T. (1989) Carbon isotope discrimination and

632   photosynthesis. *Annual Review of Plant Physiology and Plant Molecular Biology*, **40**,

633   503–537.

634   Fischer, C. & Höll, W. (1991) Food reserves of Scots pine (*Pinus sylvestris* L.). 1. Seasonal-

635   changes in the carbohydrate and fat reserves of pine needles. *Trees*, **5**, 187–195.

636   Franck, N., Vaast, P., Génard, M. & Dauzat, J. (2006) Soluble sugars mediate sink feedback

637   down-regulation of leaf photosynthesis in field-grown *Coffea arabica*. *Tree Physiology*,

638   **26**, 517–525.

639   Fritts, H.C. (2001). *Tree Rings and Climate*. Blackburn Press, Caldwell, NJ.

640   Galiano, L., Martínez-Vilalta, J. & Lloret, F. (2011) Carbon reserves and canopy defoliation

641   determine the recovery of Scots pine 4 yr after a drought episode. *New Phytologist*, **190**,

642   750–759.

643   Gillner S., Rüger N., Roloff, A. & Berger, U. (2013) Low relative growth rates predict future

644   mortality of common beech (*Fagus sylvatica* L.). *Forest Ecology and Management*, **302**,

645   372–378.

646   Grace, J.B. (2006) *Structural Equation Modeling and Natural Systems*. Cambridge University

647   Press, Cambridge.

648   Gričar, J., Krže, L. & Čufar, K. (2009). Number of cells in xylem, phloem and dormant

649   cambium in silver fir (*Abies alba*), in trees of different vitality. *IAWA Journal*, **30**, 121–

650   123.

651   Hargreaves, G.H. & Samani, Z.A. (1982) Estimating potential evapotranspiration. *Journal of*

652   *Irrigation and Drainage Engineering*, **108**, 225–230.

653   Hartmann, H., Ziegler, W., Trumbore, S. (2013) Lethal drought leads to reduction in

654   nonstructural carbohydrates in Norway spruce tree roots but not in the canopy. *Functional*

655   *Ecology*, **27**, 413–427.

656   Heiniger, U., Theile, F., Rigling, A. & Rigling, D. (2011) Blue-stain infections in roots, stems

657   and branches of declining *Pinus sylvestris* trees in a dry inner alpine valley in Switzerland.

658   *Forest Pathology*, **41**, 501–509.

659   Holmes, R.L. (1983) Computer-assisted quality control in tree–ring dating and measurement.

660   *Tree-Ring Bulletin*, **43**, 69–78.

661   Jenkins, M.A. & Pallardy, S.G. (1995) The influence of drought on red oak group species

662   growth and mortality in the Missouri Ozarks. *Canadian Journal of Forest Research*, **25**,

663   1119–1127.

664   Kõljalg, U., Larsson, K.-H., Abarenkov, K., Nilsson, R.H., Alexander, I.J., Eberhardt, U. *et*

665   *al*. (2005) UNITE: a database providing web-based methods for the molecular

666   identification of ectomycorrhizal fungi. *New Phytologist*, **166**, 1063–1068.

667   Linares, J.C. & Camarero, J.J. (2012) From pattern to process: linking intrinsic water-use

668   efficiency to drought-induced forest decline. *Global Change Biology*, **18**, 1000–1015.

669   Manion, P.D. (1991) *Tree Disease Concepts.* Prentic Hall, Englewood Cliffs.

670   McDowell, N., Pockman, W.T., Allen, C.D., Breshears, D.D., Cobb, N., Kolb, T., Plaut, J.,

671   Sperry, J., West, A., Williams, D.G. & Yepez, E.A. (2008) Mechanisms of plant survival

672   and mortality during drought: why do some plants survive while others succumb to

673   drought? *New Phytologist*, **178**, 719–739.

674   Ogle, K., Whitham, T.G. & Cobb, N.S. (2000) Tree-ring variation in pinyon predicts

675   likelihood of death following severe drought. *Ecology*, **81**, 3237–3243.

676   Oleksyn, J., Zytkowiak, R., Karolewski, P., Reich, P.B. & Tjoelker, M.G. (2000) Genetic and

677   environmental control of seasonal carbohydrate dynamics in trees of diverse *Pinus*

678   *sylvestris* populations. *Tree Physiology*, **20**, 837–847.

679   Oliva, C. & Colinas, C. (2007) Decline of silver fir (*Abies alba* Mill.) stands in the Spanish

680   Pyrenees: Role of management, historic dynamics and pathogens. *Forest Ecology and*

681   *Management*, **252**, 84–97.

682   Oliva, J., Suz, L.M. & Colinas, C. (2009) Ecology of *Armillaria* species on silver fir (*Abies*

683   *alba*) in the Spanish Pyrenees. *Annals of Forest Science*, **66**, 603.

684   Oliva, J., Stenlid, J. & Martínez-Vilalta, J. (2014) The effect of fungal pathogens on the water

685   and carbon economy of trees: implications for drought-induced mortality. *New*

686   *Phytologist* doi: 10.1111/nph.12857

687   Pasho, E., Camarero, J.J., de Luis, M. & Vicente–Serrano, S.M. (2011) Impacts of drought at

688   different time scales on forest growth across a wide climatic gradient in northeastern

689   Spain. *Agricultural and Forest Meteorology*, **151**, 1800–1811.

690   Pedersen, B.S. (1998) The role of stress in the mortality of midwestern oaks as indicated by

691   growth prior to death. *Ecology*, **79**, 79–93.

692   Peguero-Pina, J.J., Camarero, J.J., Abadía, A., Martín, E., González-Cascón, R., Morales, F.

693   & Gil-Pelegrín, E. (2007) Physiological performance of silver-fir (*Abies alba* Mill.)

694   populations under contrasting climates near the south-western distribution limit of the

695   species. *Flora*, **202**, 226–236.

696   Poyatos, R., Aguadé, D., Galiano, L., Mencuccini, M. & Martínez-Vilalta, J. (2013) Drought-

697   induced defoliation and long periods of near-zero gas exchange play a key role in

698   accentuating metabolic decline of Scots pine. *New Phytologist*, **200**, 388–401

699   R Development Core Team. (2014) *R: A language and Environment for Statistical*

700   *Computing*, version 3.0.3. R Foundation for Statistical Computing, Vienna.

701 Rodríguez-Calcerrada, J., Shahin, O., del Rey, M.C. & Rambal, S. (2011) Opposite changes

702   in leaf dark respiration and soluble sugars with drought in two Mediterranean oaks.

703   *Functional Plant Biology*, **38**, 1004–1015.

704 Ryan, M.G. & Yoder, B.J. (1997) Hydraulic limits to tree height and tree growth. *BioScience*,

705   **47**, 235–242.

706 Saffell, B.J., Meinzer F.C., Woodruff, D.R., Shaw, D.C., Voelker, S.L., Lachenbruch, B. &

707   Falk, K. (2014) Seasonal carbohydrate dynamics and growth in Douglas-fir trees

708   experiencing chronic, fungal-mediated reduction in functional leaf area. *Tree Physiology*,

709   **34**, 218–228.

710 Sala, A., Piper, F. & Hoch, G. (2010) Physiological mechanisms of drought induced tree

711   mortality are far from being resolved. *New Phytologist*, **186**, 274–281.

712 Sangüesa-Barreda, G., Linares, J.C. & Camarero, J.J. (2013) Drought and mistletoe reduce

713   growth and water-use efficiency of Scots pine. *Forest Ecology and Management*, **296**, 64–

714   73.

715 Scheffer, M., Carpenter, S.R., Foley, J.A., Folke, C. & Walker, B. (2001) Catastrophic shifts

716   in ecosystems. *Nature*, **413**, 591–596.

717 Secchi, F. & Zwieniecki, M.A. 2012. Analysis of xylem sap from functional (nonembolized)

718   and nonfunctional (embolized) vessels of *Populus nigra*: chemistry of refilling. *Plant*

719   *Physiology*, 160, 965–994.

720 Sevanto, S., McDowell, N.G., Dickman, L.T., Pangle, R. & Pockman, W.T. (2014) How do

721   trees die? A test of the hydraulic failure and carbon starvation hypotheses. *Plant, Cell*

722   *and Environment*, **37**, 153–161.

723 Smith, M.D. (2011) An ecological perspective on extreme climatic events: a synthetic

724   definition and framework to guide future research. *Journal of Ecology*, **99**, 656–663.

725 Vicente-Serrano, S.M., Beguería, S. & López-Moreno, J.I. (2010) A multiscalar drought

726   index sensitive to global warming: the standardized precipitation evapotranspiration

727   index. *Journal of Climate*, **23**, 1696–1718.

728 Vicente-Serrano, S.M., Gouveia, C., Camarero, J.J., Beguería, S., Trigo, R., López-Moreno,

729   J.I. et al. (2013) Response of vegetation to drought time–scales across global land

730   biomes. *Proceedings of the National Academy of Sciences of the United States of*

731   *America*, **110**, 52–57.

732 Voltas, J., Camarero , J.J., Carulla, D., Aguilera, M., Ortiz, A. & Ferrio, J.P. (2013) A

733   retrospective, dual-isotope approach reveals individual predispositions to winter-drought

734   induced tree dieback in the southernmost distribution limit of Scots pine. *Plant, Cell and*

735   *Environment*, **36**, 1435–1448.

736 Williams, A.P., Allen, C.D., Macalady, A.K., Griffin, D., Woodhouse, C.A., Meko, D.M., et

737   al. (2013) Temperature as a potent driver of regional forest drought stress and tree

738   mortality. *Nature Climate Change*, **3**, 292–297.

739 Wood, S.N. (2006) *Generalized Additive Models: An Introduction with R*. Chapman and

740   Hall/CRC Press, Boca Raton.

741 Wood, S.N. (2011) Fast stable restricted maximum likelihood and marginal likelihood

742   estimation of semiparametric generalized linear models. *Journal of the Royal Statistical*

743   *Society: Series B*, **73**, 3–36.

744 Woodall, C.W. (2008) When is one core per tree sufficient to characterize stand attributes?

745   Results of a *Pinus ponderosa* case study. *Tree-Ring Research*, **64**, 50–60.

746

Tables

748 **Table 1. Main features of the three study sites and tree species. Values are means ± SE.**

Site	Paco Ezpela	El Carrascal	Vedado de Peñaflor
Species	*Abies alba* Mill.	*Pinus sylvestris* L.	*Pinus halepensis* Mill.
Latitude (N)	42º 45'	40º 26'	41º 47'
Longitude (W)	0º 52'	0º 58'	0º 44'
Elevation (m a.s.l.)	1230	1303	375
Aspect	NE	NW	NE
Slope (º)	35	25	5
Soil type, soil texture	Cambisol, loamy	Cambisol, loamy	Regosol, loamy
Soil pH	7.1	7.7	8.1
Annual water balance (mm) [1]	531	−210	−468
No. trees	38	38	38
No. dead trees pre- / post-drought [2]	8 / 16	7 / 25	4 / 7
No. non-declining / declining trees [2]	23 / 12	13 / 24	19 / 14
No. trees with tree-ring data	35	37	33
Distance to nearest sampled tree (m)	10.6 ± 1.5	8.5 ± 1.3	29.2 ± 4.8
Dbh (cm) [3]	37.3 ± 1.2	27.3 ± 1.0	32.3 ± 1.4
Height (m)	24.0 ± 0.5	8.5 ± 0.3	7.8 ± 0.3
Age (years) [4]	85 ± 3	138 ± 6	94 ± 4
Crown cover (%)	59.9 ± 5.9	58.0 ± 4.9	55.4 ± 4.7
Sapwood area (%)	15.2 ± 2.2	8.6 ± 1.2	17.0 ± 2.8
Frequency of trees severely infested by mistletoe (%) [5]	29	0	29
Basal area (m^2 ha^{-1})	18	15	8
Tree-ring width for period 1950−2012 (mm)	2.00 ± 0.02	0.40 ± 0.01	0.85 ± 0.02
Main co-occurring tree species	*Fagus sylvatica* L.	*Pinus nigra* subsp. *salzmannii* (Dunal) Franco	*Juniperus thurifera* L.
Climatic station (distance to sampling site in km)	Jaca, 42° 34' N, 0° 33' W, 818 m (30)	Teruel, 40° 21' N, 1° 06' W, 915 m (15)	Zaragoza, 41° 39' N, 0° 53' W, 208 m (24)

749

750 [1]The water balance is defined as the difference between precipitation and potential evapotranspiration.

751 [2] Dead trees were regarded as those completely defoliated or having only red needles at the end of the drought.

752 Non-declining trees were considered those presenting post-drought defoliation of < 50%; declining trees were

753 considered those presenting post-drought defoliation of ≥50%. These trees were counted after the 2012 drought.

754 [3]Diameter at breast height (dbh) measured at 1.3 m.

755 [4]Age estimated at 1.3 m.

756 [5]Trees with abundant mistletoe individuals growing in at least one-third of the crown.

757

758

759

Table 2. Comparison of relevant variables calculated for declining and non-declining trees in the three study species and based on *t* tests (significant *t* values with *P* < 0.05 are in bold; negative *t* values indicate higher value of variables for declining than for non-declining trees and vice versa). Values are means ± SE.

Species	Variable	Declining trees	Non-declining trees	*t*	*P*
Abies alba	Dbh (cm)	26.97 ± 1.45	27.70 ± 1.33	0.35	0.730
	Height (m)	8.62 ±0.48	8.58 ± 0.42	−0.05	0.962
	Defoliation (%)	78.23 ± 4.41	21.46 ± 2.26	**−12.75**	<0.0001
	Sapwood length (cm)	3.17 ±0.33	5.91 ± 0.35	**2.09**	0.045
	Age (years)	146 ±11	133 ± 7	−0.97	0.336
	Post-drought sapwood SS (%)	0.29 ± 0.02	0.39 ± 0.01	**2.08**	0.046
	BAI 2008−2012 (cm^2)	1.65 ± 0.37	3.51 ± 0.41	**2.97**	0.005
	No. expanding tracheids	3 ± 1	10 ± 2	**6.88**	<0.0001
Pinus sylvestris	Dbh (cm)	36.93 ± 1.89	36.36 ± 1.64	−0.21	0.833
	Height (m)	24.13 ±0.97	23.41 ± 0.66	−0.62	0.540
	Defoliation (%)	87.92 ± 5.82	18.83 ± 2.38	**−13.00**	<0.001
	Sapwood length (cm)	2.50 ± 0.60	7.70 ± 0.68	**5.02**	0.001
	Age at 1.3 m (years)	91 ± 4	88 ± 3	−0.51	0.615
	Post-drought sapwood SS (%)	0.21 ± 0.02	0.30 ± 0.01	**4.22**	0.001
	BAI 2008−2012 (cm^2)	3.41 ± 0.78	12.02 ± 1.33	**4.44**	0.001
	No. expanding tracheids	3.5 ± 0.8	4.1 ± 1.9	1.51	0.136
Pinus halepensis	Dbh (cm)	29.03 ± 2.70	34.12 ± 1.57	1.73	0.094
	Height (m)	7.56 ± 0.55	7.95 ± 0.35	0.63	0.535
	Defoliation (%)	70.14 ± 4.39	26.21 ± 3.74	**−7.63**	<0.001
	Sapwood length (cm)	4.57 ± 0.73	6.68 ± 0.68	**2.09**	0.045
	Age at 1.3 m (years)	78 ± 5	93 ± 6	1.83	0.072
	Post-drought sapwood SS (%)	0.63 ± 0.06	0.79 ± 0.04	**2.24**	0.033
	BAI 2008−2012 (cm^2)	0.12 ± 0.08	1.20 ±0.41	**2.20**	0.036
	No. expanding tracheids	2.6 ± 0.9	3.5 ± 1.7	1.56	0.123

BAI, basal area increment; dbh, diameter at breast height; SS, soluble sugars.

Table 3. Models selected to explain yearly log-transformed basal area increment [log (BAI+1)] of declining and non-declining trees as a function of smoothing terms (s) and interactions (*). Two models are shown for each species. The first model was fitted by selecting the best structural model, including only trend, tree diameter (dbh) and age and spatial coordinates. Eight potential models were compared and the best one was selected according to the ΔAIC (difference in AIC between the best and the second-best model). The second model was fitted including the best first model, the influence of summer drought (June SPEI calculated at 5- and 10-month-long scales) and the potential difference in growth, trend and response to drought of non-declining vs. declining trees. Nine potential models were compared and the best one was selected according to the ΔAIC (difference in AIC between the best and the second-best model). The adjusted R^2 of each model is also shown. The non-linear and linear coefficients of the second-best model are shown in Tables S2 and 4 respectively. The adjusted bai of the second-best model is shown in Figure 6.

Species	No. rings	Models	AIC	ΔAIC	Adj R^2
Abies alba	2142	s(year) + s(dbh)	373	3.8	0.39
		s(year * declining) + s(dbh) + declining + June SPEI$_5$	320	1.3	0.48
Pinus sylvestris	2327	s(year) + s(dbh) + s(age)	2397	3.9	0.52
		s(year * declining) + s(age) s(dbh)+ declining * June SPEI$_5$	2083	1.6	0.58
Pinus halepensis	1974	s(year)	1286	1.1	0.32
		s(year) + declining * June SPEI$_{10}$	698	2.0	0.39

AIC, Akaike information criterion; dbh, diameter at breast height; GAMM, generalized additive mixed models; SPEI, standardized precipitation–evapotranspiration index.

789 **Table 4. Linear terms of the second-best model (see abbreviations and symbols for**

790 **variables in Tables 2 and 3). For each species the associated coefficient of each linear**

791 **predictor (SE), the *t*-statistic and its probability (*P*) value are shown.**

792

Species	Model	Coefficient	SE	t	P
Abies alba	Non-declining vs. declining	0.17	0.09	1.96	0.048
	June $SPEI_5$	0.03	0.01	5.12	<0.001
	Non-declining * June $SPEI_5$	–	–	–	–
Pinus sylvestris	Non-declining vs. declining	0.26	0.14	1.84	0.053
	June $SPEI_5$	0.13	0.01	9.58	<0.001
	Non-declining * June $SPEI_5$	0.03	0.02	1.89	0.059
Pinus halepensis	Non-declining vs. declining	0.11	0.07	1.53	0.127
	June $SPEI_{10}$	0.12	0.01	15.55	<0.001
	Non-declining * June $SPEI_{10}$	0.02	0.01	2.23	0.026

793

794
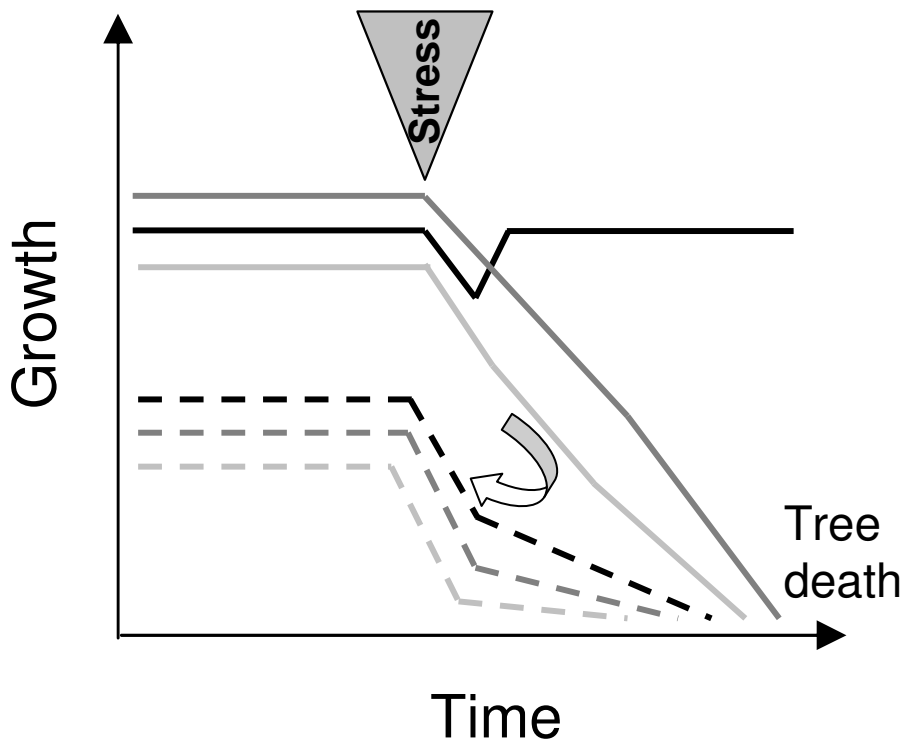
Figures

Figure 1. A conceptual model of tree mortality based on the tipping-point concept where the arrow indicates a post-drought critical transition (tipping point) from non-declining to declining growth trajectories in response to a stress factor such as a drought (modified from Pedersen 1998 and Manion 1991). Solid lines represent non-declining trees; broken lines represent declining trees. Both types of tree can die (no growth) showing diverse rates and paces of growth reduction after a stress event (inciting factor *sensu* Manion 1991) such as a severe drought. The arrow indicates a post-drought critical transition from non-declining to declining growth trajectories.

807
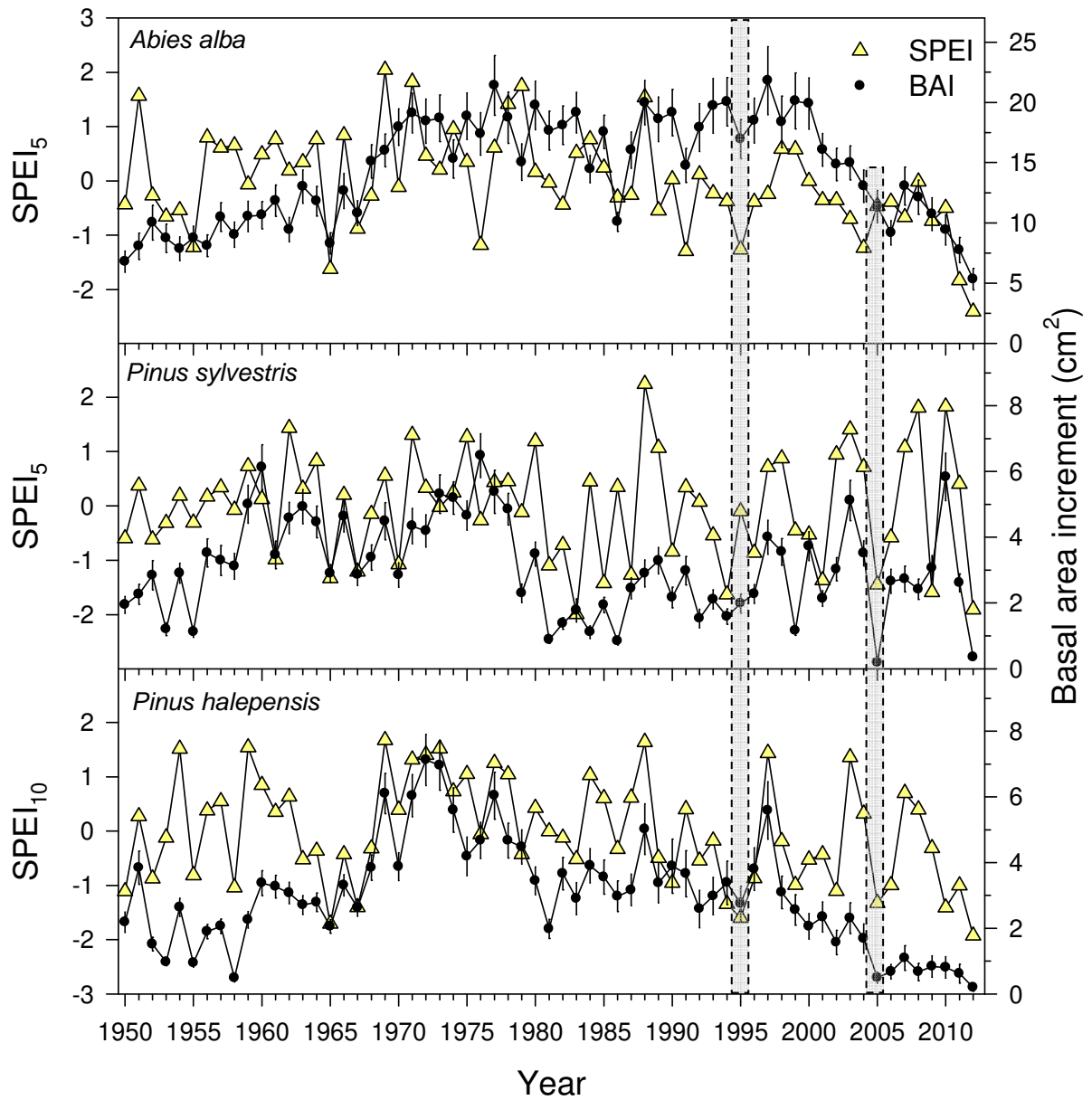
Figure 2. Growth patterns (mean basal area increment ± SE) of the three study species as related to drought severity: June Standardized Precipitation−Evapotranspiration Index calculated at scales of 5 (SPEI₅) for *A. alba* and *P. sylvestris* or 10 months (SPEI₁₀) for *P. halepensis*. The vertical grey boxes indicate the severe 1995 and 2005 droughts.

812

813

814
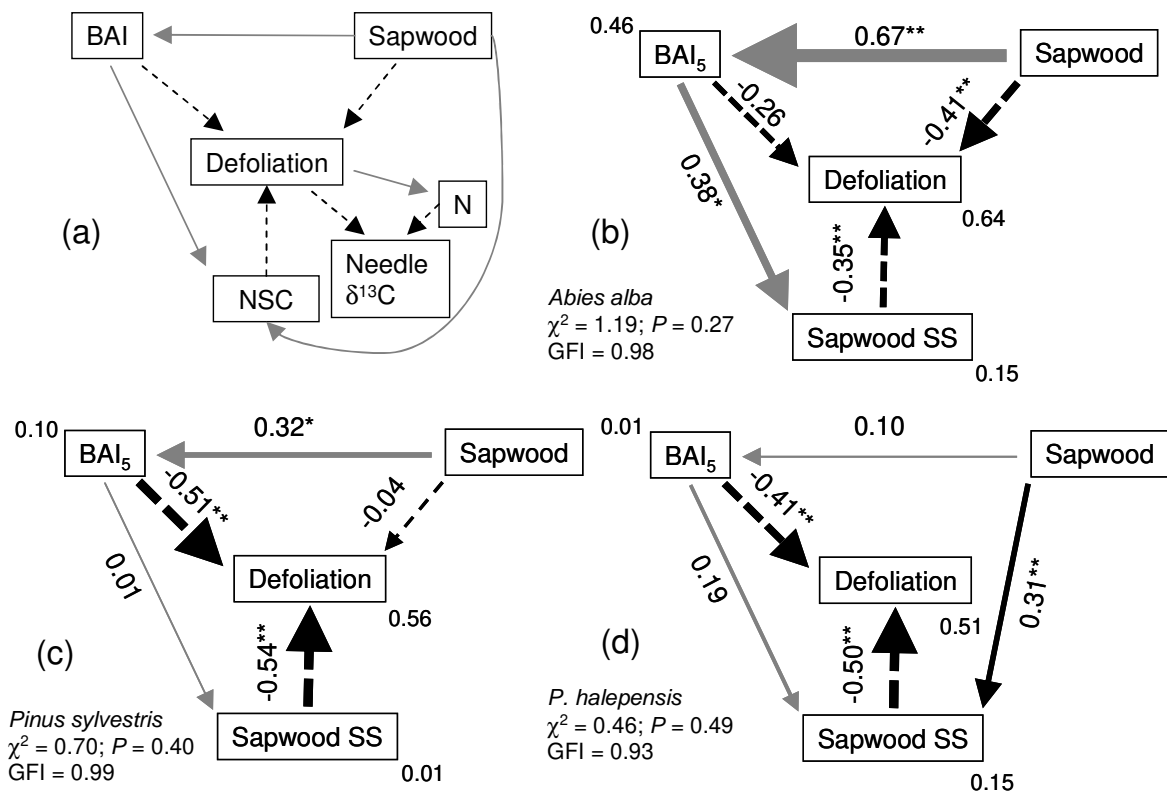
Figure 3. Conceptual functional model of tree decline (a) relating different variables (BAI$_5$,
basal area increment of the previous five years; sapwood length; N, needle N concentration;
δ^{13}C, needle carbon isotopic discrimination; NSC, total non-structural carbohydrate
concentrations in sapwood or needles) and structural equation models (SEM) fitted to silver
fir (*Abies alba*) (b), Scots pine (*Pinus sylvestris*) (c) and Aleppo pine (*Pinus halepensis*) (d)
trees. The broken and solid arrows indicate negative and positive relationships (significance
levels are *P<0.05 and **P<0.01). Arrow sizes are proportional to the magnitude of
standardized path coefficients (numbers located above arrows). Explained variance of each
observed variable is indicated in corners near boxes. In each SEM, three fitting statistics are
shown in the lower left inset (χ^2 statistic and its corresponding P value; GFI, Goodness of Fit
Index). Note that some variables shown in the conceptual model were not selected in the fitted
models or were only available for some of the study species (e.g. mistletoe abundance or
presence of fungi).
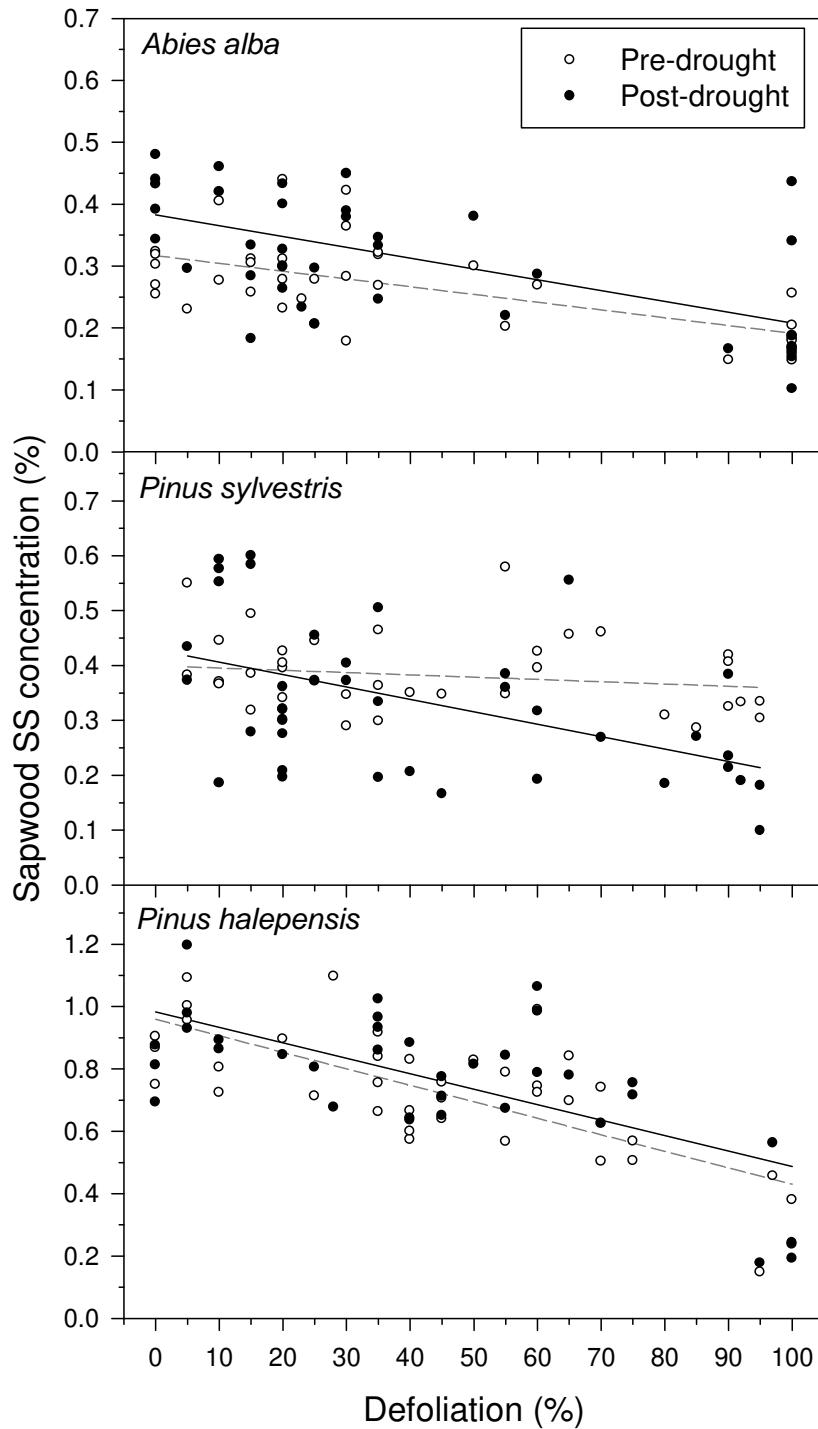
828
829
830
831 **Figure 4.** Negative associations observed for the three study species between tree defoliation

832 and the concentration of soluble sugars (SS) in the sapwood before and after a severe drought

833 event (see also Fig. 2). All relationships are highly significant ($P<0.01$) apart from the one

834 corresponding to the pre-drought period in Scots pine ($r = −0.18$, $P = 0.28$).

835

836
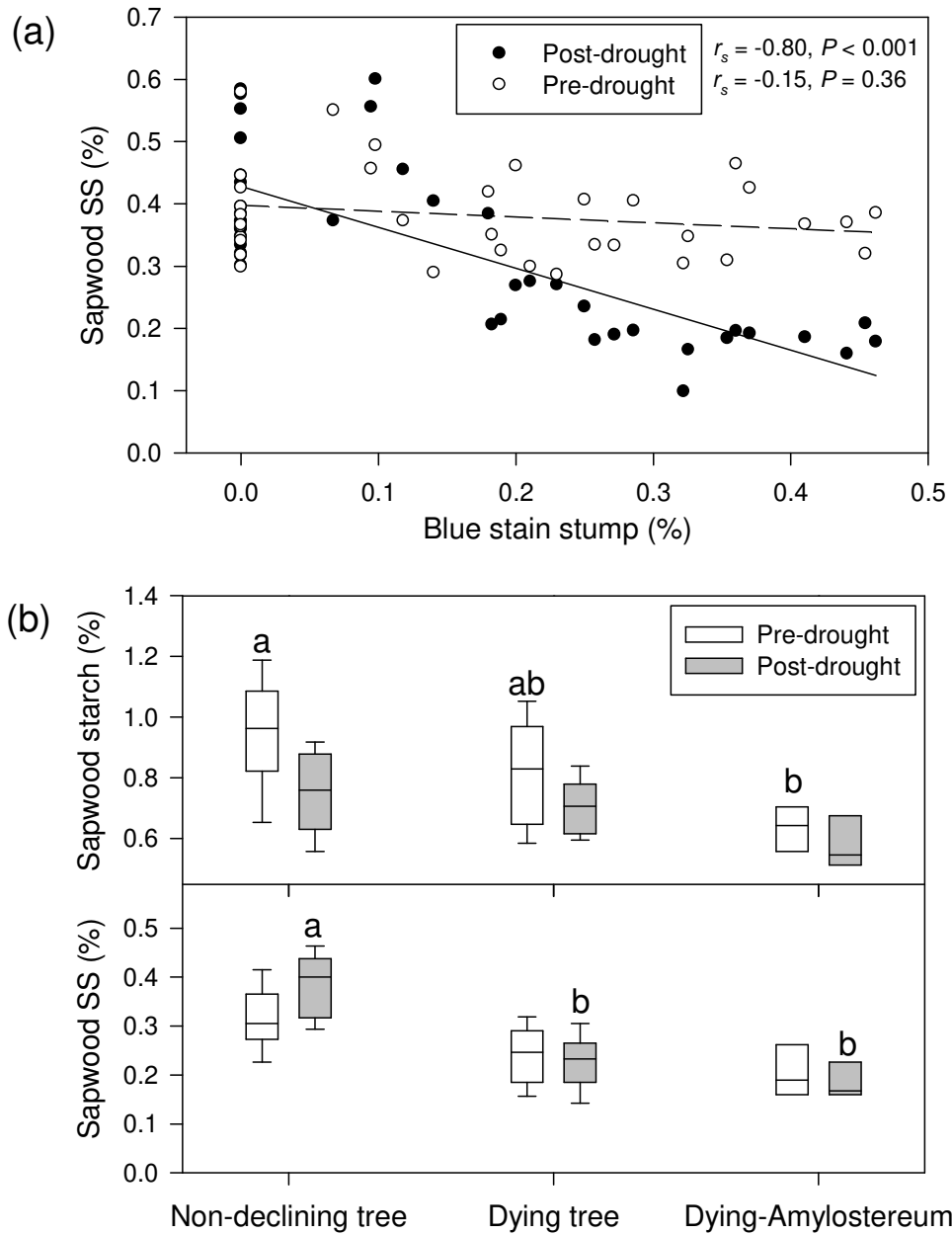
Figure 5. Main findings relating to tree vigour, sapwood non-structural carbohydrate

concentrations (starch and soluble sugars, SS) before and after drought and presence of fungi

in *Pinus sylvestris* (a) and *Abies alba* (b). In (a), the relationships between variables are

described using the Spearman correlation coefficient (r_s). In (b), different letters indicate

significant differences between tree types within each season (pre- or post-drought

comparisons) according to Tukey HSD tests.

843
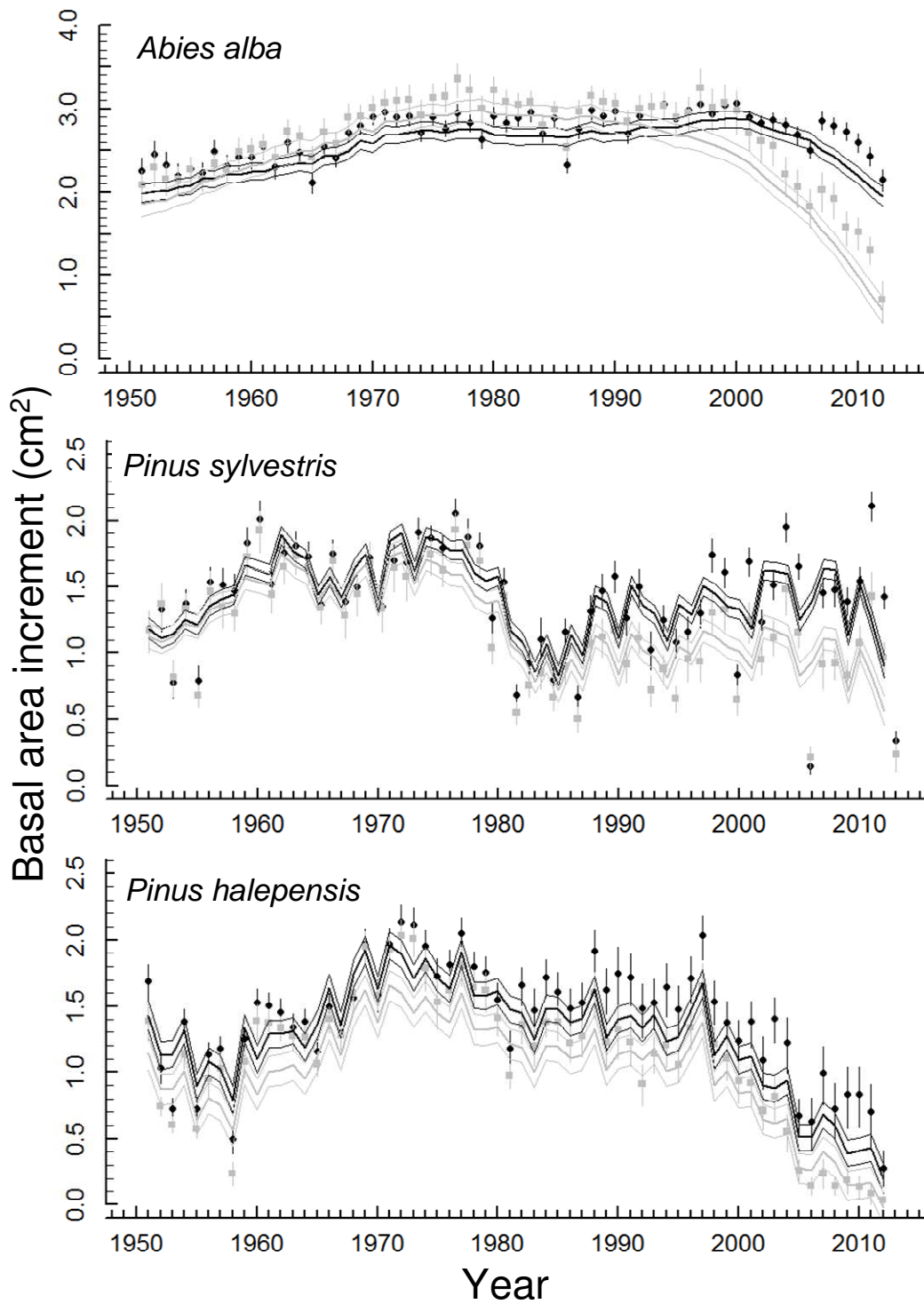
Figure 6. Observed (symbols with error bars) and modelled (log-transformed) basal-area

increment trends (mean ± SEs are shown) for declining (grey symbols and lines) and non-

declining (black symbols and lines) silver fir (*A. alba*), Scots pine (*P. sylvestris*) and Aleppo

pine (*P. halepensis*) trees. Trends were based on the best-fitted generalized additive mixed

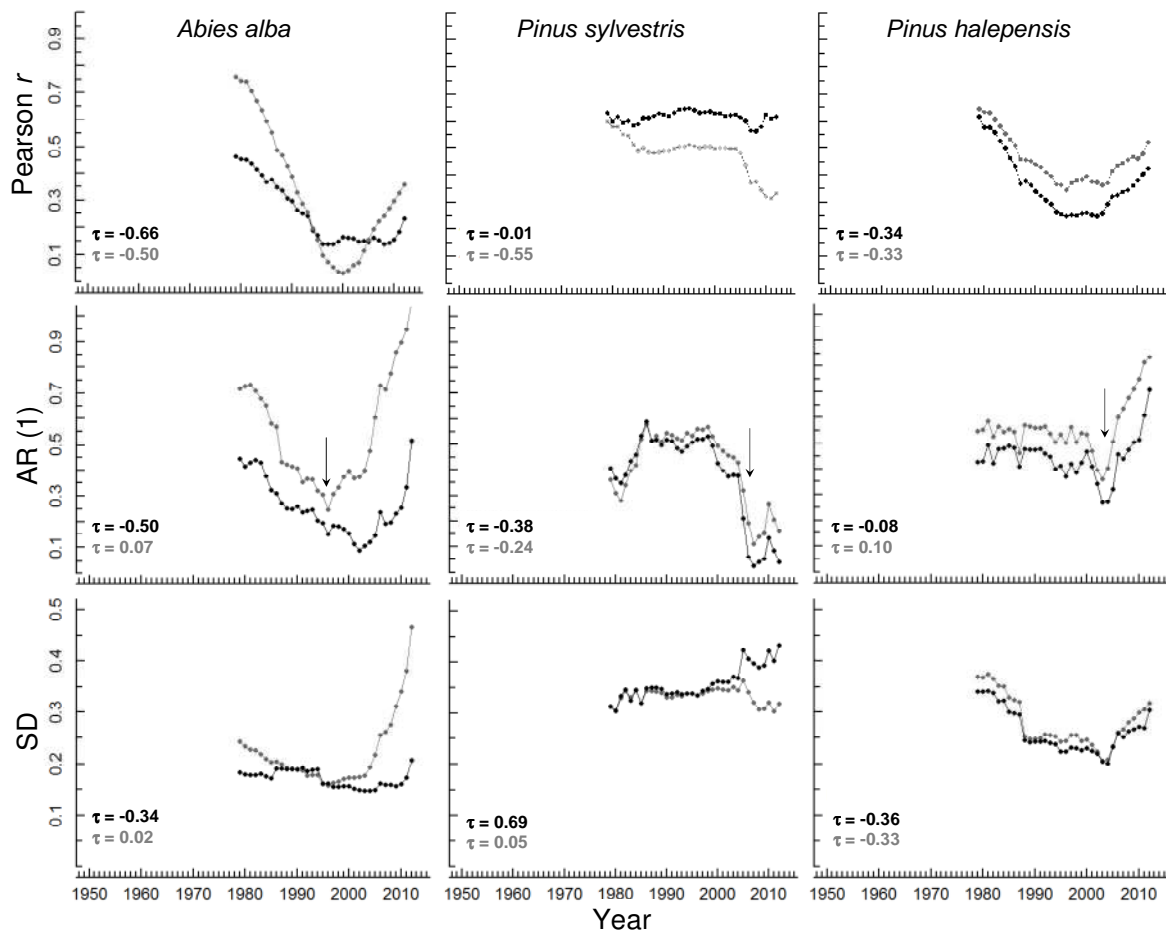models for the period 1950–2012 (see statistical parameters in Table 3).

Figure 7. Early-warning signals (moving Pearson correlations; AR(1), first-order autocorrelation; SD, standard deviation) obtained using 30-year moving windows for basal-area increment (bai) series of declining (grey lines) and non-declining trees (black lines) of the three study species (*A. alba*, *P. sylvestris* and *P. halepensis*). The statistics were calculated for bai individual series (upper graphs) or bai residuals of mean series for declining and non-declining trees (middle and lower graphs) after extracting mid-term trends using 30-year-long windows. The symbols correspond to the last year of each 30-year interval (e. g, 1979 corresponds to the interval 1950−1979). The Kendall τ statistics indicate the trends for each variable. The arrows indicate severe droughts in 1995 and 2005 (see Fig. 1).

Supporting Information

Table S1. Dendrochronological statistics (means ± SE) of the tree-ring width series.

Species	No. trees	First-last years	Tree-ring width (mm)	Correlation with mean series	First-order autocorrelation	Mean sensitivity[1]
Abies alba	35	1886-2012	1.99 ± 0.11	0.59 ± 0.02	0.23 ± 0.01	0.22 ± 0.01
Pinus sylvestris	37	1817-2012	0.70 ± 0.04	0.78 ± 0.02	0.62 ± 0.02	0.49 ± 0.01
Pinus halepensis	33	1869-2012	1.05 ± 0.08	0.73 ± 0.02	0.68 ± 0.02	0.44 ± 0.01

[1]A measure of the year-to-year variability in width of consecutive tree rings (Fritts 2001).

Table **S2**. Sensitivity analysis calculated for selected variables (BAI, basal area increment) showing significant differences when comparing declining vs. non-declining trees using two thresholds to classify trees according to their defoliation (40% and 60%). Overall, we observed similar results when using the aforementioned defoliation thresholds and comparing the variable as when considering the 50% defoliation threshold (see Table 2), except two variables in the case of *P. halepensis* (bold values shown in the table).

Species	Variable	40% defoliation threshold		60% defoliation threshold	
		t	P	t	P
Abies alba	Defoliation (%)	−11.31	<0.0001	−11.78	<0.0001
	Sapwood length (cm)	2.35	0.024	2.28	0.031
	BAI 2008−2012 (cm^2)	3.34	0.002	3.56	0.001
Pinus sylvestris	Defoliation (%)	−13.00	<0.001	−14.07	<0.001
	Sapwood length (cm)	5.01	0.001	4.23	0.001
	BAI 2008−2012 (cm^2)	4.44	0.001	3.84	0.001
Pinus halepensis	Defoliation (%)	−7.04	<0.001	−7.08	<0.001
	Sapwood length (cm)	2.05	0.048	1.54	**0.133**
	BAI 2008−2012 (cm^2)	2.64	0.013	1.49	**0.147**

Negative and positive *t* values indicate higher values for declining and non-declining trees, respectively.

Table S3. Statistical parameters of the non-linear terms of the second best GAMM fitted to basal area increment of declining and non-declining trees (see Table 2). For each species (*P. sylvestris, A. alba and P. halepensis*) the degrees of freedom of the smooth term (edf), the associated *F* statistic and the *P* value of each selected term are shown.

Species	Terms	edf	*F*	*P*
Pinus sylvestris	Trend (year) declining	7.88	30.77	<0.001
	Trend (year) non-declining	8.63	28.64	<0.001
	age	3.25	12.20	<0.001
	dbh	1.00	51.32	<0.001
	Spatial location	–	–	–
Abies alba	Trend (year) declining trees	6.02	27.73	<0.001
	Trend (year) non-declining trees	6.65	11.12	<0.001
	age	–	–	–
	dbh	1.00	67.32	<0.001
	Spatial location	–	–	–
Pinus halepensis	Trend (year)	8.29	46.31	<0.001
	age	–	–	–
	dbh	–	–	–
	Spatial location	–	–	–

Figure S1. Illustrative views of drought-induced dead or dying silver fir (*Abies alba*, a), Scots pine (*Pinus sylvestris*, b) and Aleppo pine (*Pinus halepensis*, c) stands and trees.
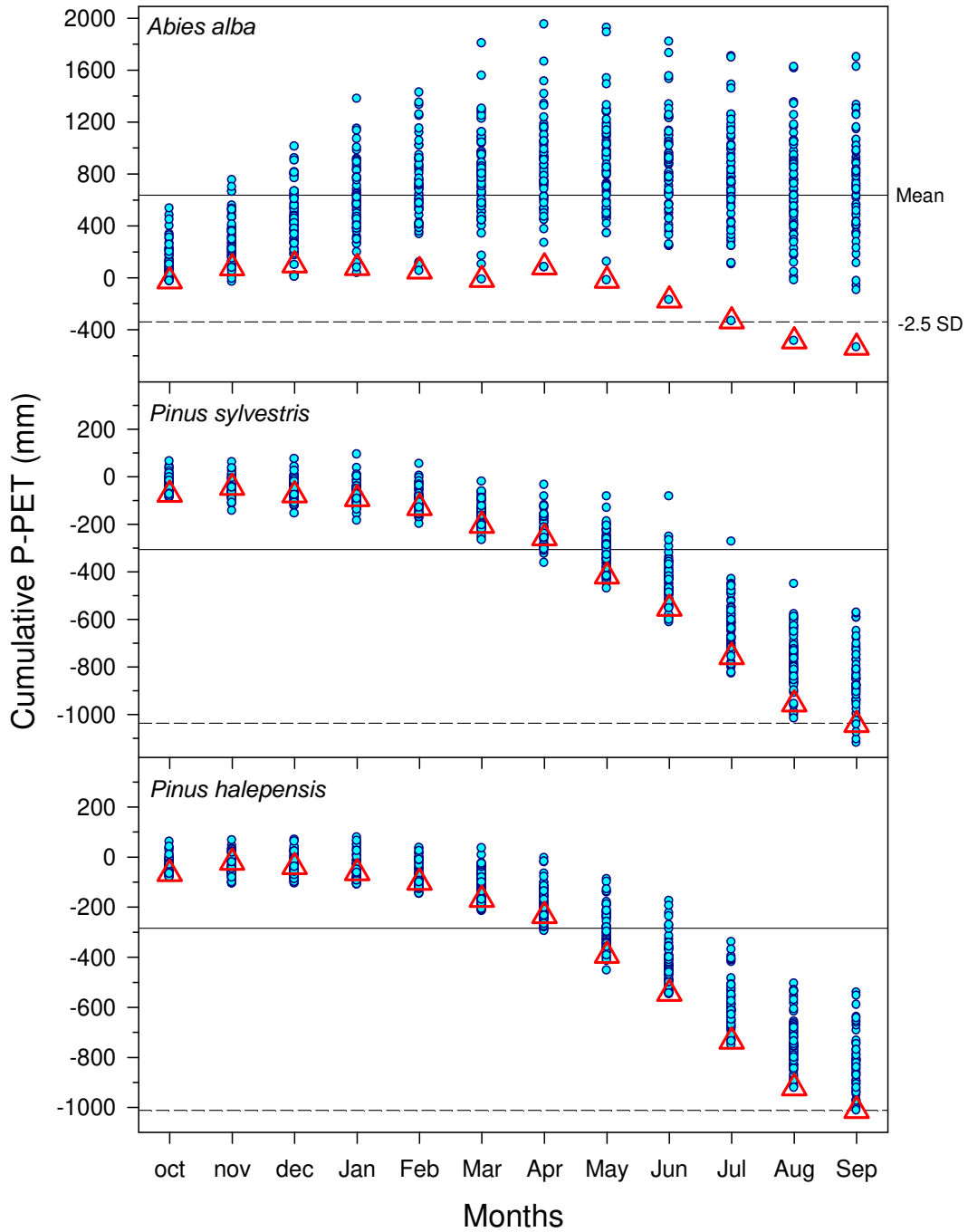
Figure S2. Monthly cumulative water balance (P-PET, difference between precipitation and potential evapotranspiration) estimated for the three study species and calculated from the year prior to growth (months abbreviated by lowercase letters) up to the end of the growing season in 2012 (months abbreviated by uppercase letters). Data correspond to the period 1951−2012. The triangles show the 2012 drought while the solid and broken horizontal lines show the mean and the mean minus two times the standard deviation (−2.5 SD), respectively.
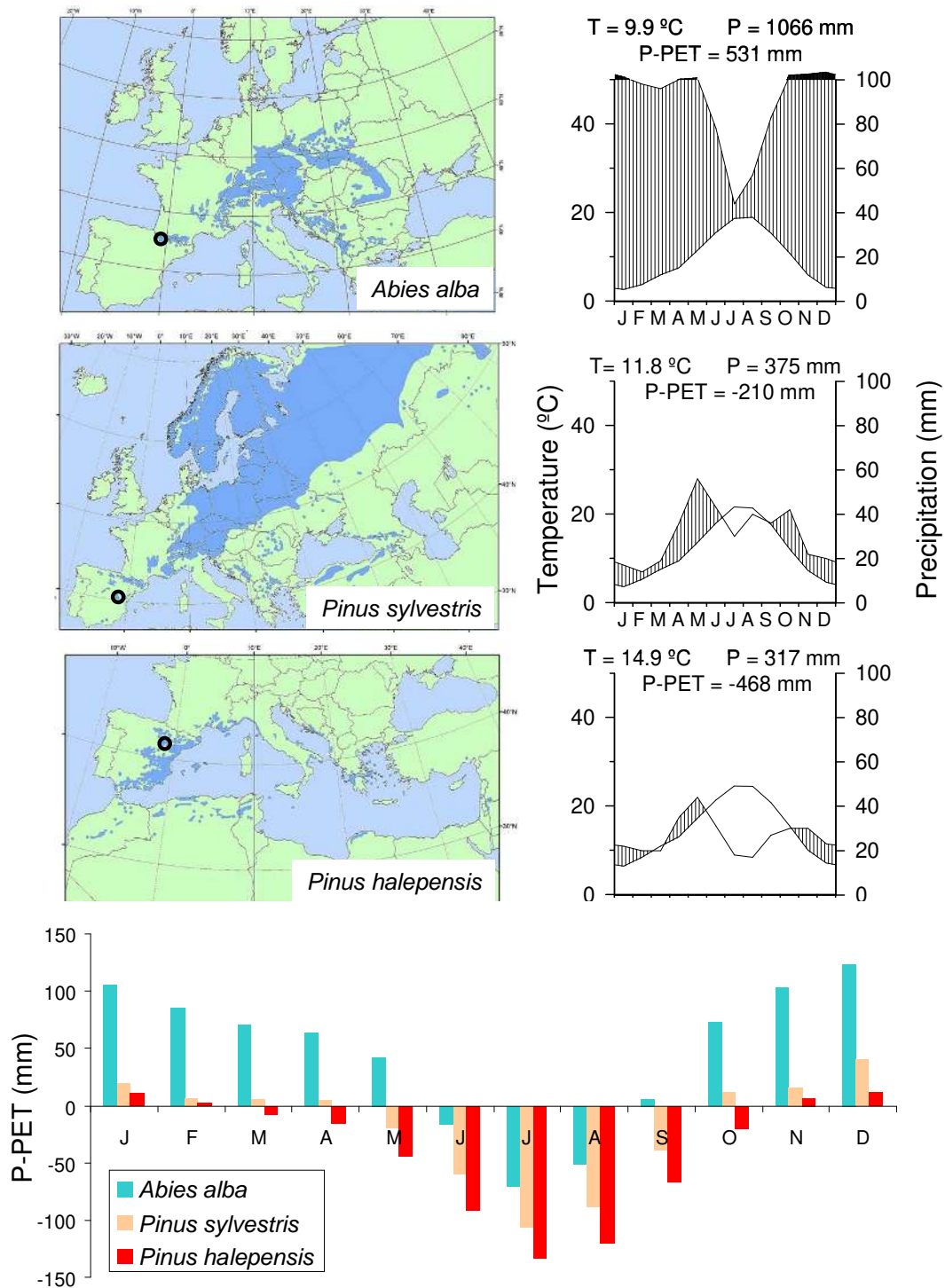
Figure S3. Geographical location (maps modified from those available at
http://www.euforgen.org/distribution_maps.html) and climatic characteristics (climatic
diagrams, water balance or difference between precipitation –P– and potential
evapotranspiration –PET) of the three study sites. Mean (T, temperature) or total (P, PET
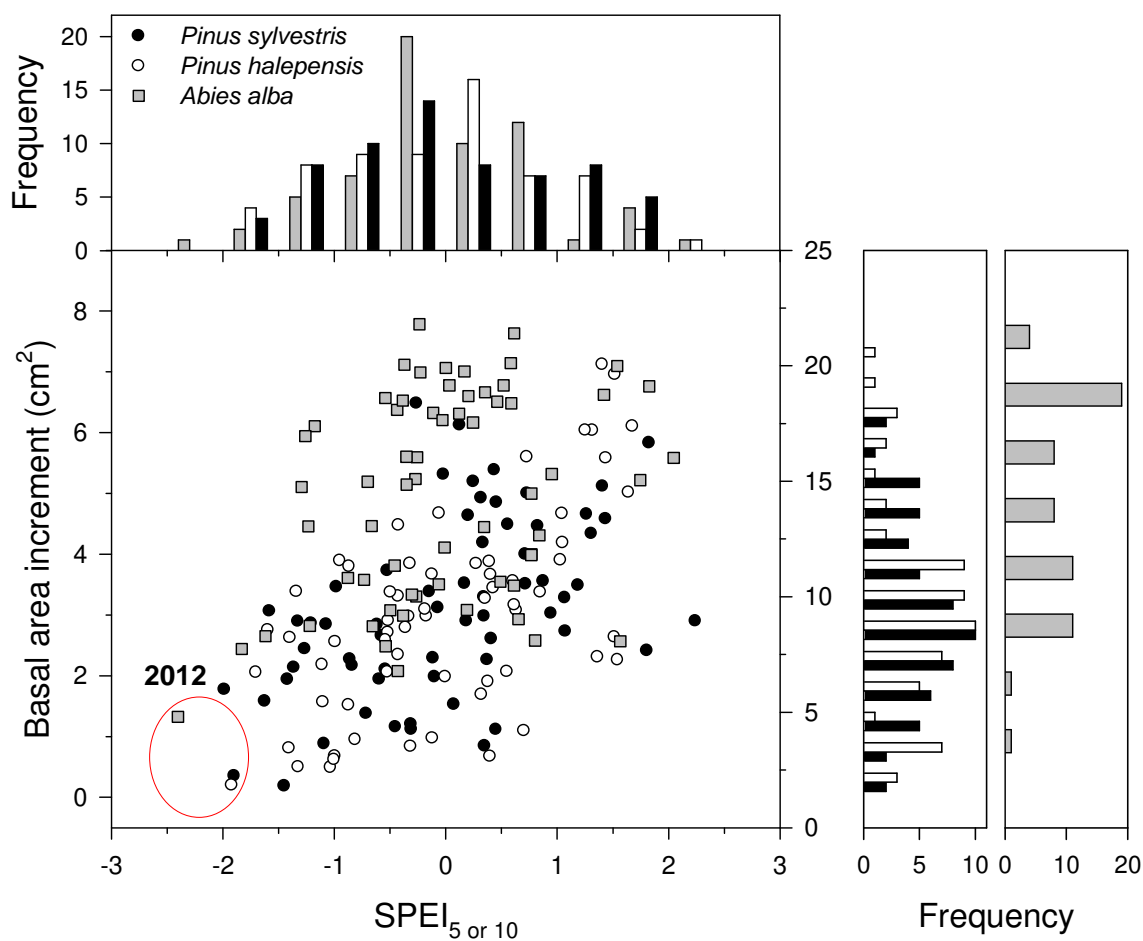lower line) annual values are indicated for each climatic diagram.

Figure S4. Relationships between mean basal area increment (BAI) of the three study species (different symbols and fill colours) and the June 5-months (*A. alba*, *P. sylvestris*) or 10-months (*P. halepensis*) long Standardised Precipitation−Evapotranspiration Index (SPEI). The histograms show the distributions of the BAI and SPEI values. The ellipse emphasizes the extreme BAI and SPEI values corresponding to the 2012 drought event.
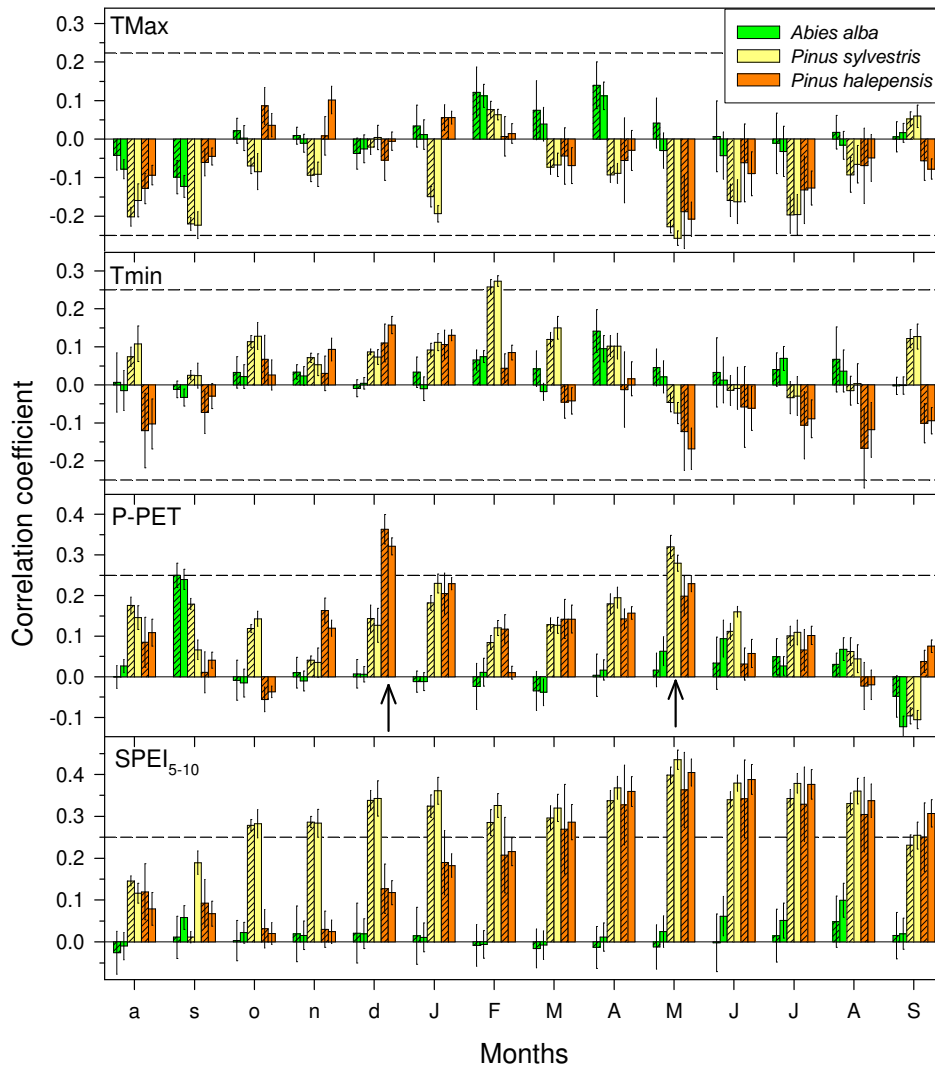
Figure S5. Associations (Pearson correlation coefficients, means ± SE) calculated between individual growth series (basal-area increment residuals) and monthly climatic variables (TMax, mean maximum temperature; Tmin, mean minimum temperature; P-PET, water balance or difference between precipitation and potential evapotranspiration; SPEI$_{5-10}$, Standardised Precipitation–Evapotranspiration Index calculated at scales of 5 −*A. alba*, *P. sylvestris*− or 10 months −*P. halepensis*) for declining (hatched bars) and non-declining (empty bars) trees of the three study species. Correlations were obtained for months prior to the year of growth (abbreviated by lowercase letters) and for months corresponding to the year of tree-ring formation (abbreviated by uppercase letters). The arrows indicate the climatic variables showing significantly (*P*<0.05) different impacts of climatic variables on growth of declining and non-declining trees for each tree species. Dashed horizontal lines show the 0.05 significance thresholds.